

Anthocyanin contribution to chlorophyll meter readings and its correction

Jan Hlavinka · Jan Nauš · Martina Špundová

Received: 24 April 2013 / Accepted: 26 September 2013 / Published online: 16 October 2013
© Springer Science+Business Media Dordrecht 2013

Abstract Leaf chlorophyll content is an important physiological parameter which can serve as an indicator of nutritional status, plant stress or senescence. Signals proportional to the chlorophyll content can be measured non-destructively with instruments detecting leaf transmittance (e.g., SPAD-502) or reflectance (e.g., showing normalized differential vegetation index, NDVI) in red and near infrared spectral regions. The measurements are based on the assumption that only chlorophylls absorb in the examined red regions. However, there is a question whether accumulation of other pigments (e.g., anthocyanins) could in some cases affect the chlorophyll meter readings. To answer this question, we cultivated tomato plants (*Solanum lycopersicum* L.) for a long time under low light conditions and then exposed them for several weeks (4 h a day) to high sunlight containing the UV-A spectral region. The senescent leaves of these plants evolved a high relative content of anthocyanins and visually revealed a distinct blue color. The SPAD and NDVI data were collected and the spectra of diffusive transmittance and reflectance of the leaves were measured using an integration sphere. The content of anthocyanins and chlorophylls was measured analytically. Our results show that SPAD and NDVI measurement can be significantly affected by the accumulated anthocyanins in the leaves with relatively high anthocyanin content. To describe theoretically this effect of anthocyanins, concepts of a specific absorbance and a leaf

spectral polarity were developed. Corrective procedures of the chlorophyll meter readings for the anthocyanin contribution are suggested both for the transmittance and reflectance mode.

Keywords Anthocyanins · Chlorophyll · Chlorophyll meters · Correction · NDVI · SPAD

List of symbols

| | |
|------------------------------------|--|
| a, b, d | Constant numbers |
| A_{535}, A_{640} | Absorbance of the sample at 535 and 640 nm, respectively |
| ACN | Anthocyanins |
| C_{ACN} | Anthocyanin content in leaf disk [nmol cm^{-2}] estimated analytically |
| C_{CHL} | Chlorophyll $a+b$ content in leaf disk [nmol cm^{-2}] estimated analytically |
| C_{Rb}, C_{Rc} | Mean theoretical anthocyanin (b) or chlorophyll (c) molar concentration [M] along the reflection pathway, respectively |
| C_{Tb}, C_{Tc} | Mean theoretical anthocyanin (b) or chlorophyll (c) molar concentration [M] along the transmission pathway, respectively |
| $D_R(\lambda)$ | Overall specific RM absorbance at λ |
| $D_{Rb}(\lambda), D_{Rc}(\lambda)$ | Specific RM absorbance of anthocyanin (b) or chlorophyll (c) at λ , respectively |
| $D_{Rg}(\lambda)$ | Mean normalized specific RM absorbance of a leaf without anthocyanins at λ |

J. Hlavinka · J. Nauš · M. Špundová (✉)
Department of Biophysics, Centre of the Region Haná for Biotechnological and Agricultural Research, Faculty of Science, Palacký University, Olomouc, Šlechtitelů 11, 78371 Olomouc, Czech Republic
e-mail: martina.spundova@upol.cz

| | | | |
|--|---|--|--|
| $D_{Rr}(\lambda)$ | Specific RM absorbance caused by reflection, scatter, refraction, and diffraction at λ | l | Confidential proportionality coefficient which defines the relative SPAD units |
| $D_T(\lambda)$ | Overall specific TM absorbance at λ | λ_{IR}, λ_R | Wavelength in the infrared (IR) and red (R) region |
| $D_{Tb}(\lambda), D_{Tc}(\lambda)$ | Specific TM absorbance of anthocyanins (b) or chlorophyll (c) at λ , respectively | $\lambda_{1R}, \lambda_{2R}, \lambda_{1T}, \lambda_{2T}$ | Detection wavelengths for the reflectance (R) and transmittance (T) mode |
| $D_{Tg}(\lambda)$ | Mean normalized specific TM absorbance of a leaf without anthocyanins at λ | $NDVI$ | Normalized difference vegetation index |
| $D_{Tr}(\lambda)$ | Specific TM absorbance caused by reflection, scatter, refraction, and diffraction at λ | $NDVI_C$ $R_m(\lambda)$ | Corrected value of $NDVI$ Measured leaf diffusive reflectance at λ |
| $D_{sR}(\lambda)$ | Calculated specific RM absorbance at λ | $R_e(\lambda), R_i(\lambda)$ | External (surface) or internal reflectance of the leaf at λ , respectively |
| $D_{sT}(\lambda)$ | Calculated specific TM absorbance at λ | $SPAD$ $SPAD_C$ | SPAD value Corrected SPAD value |
| $A_b(SPAD)$ | Relative contribution of anthocyanins (b) to the SPAD signal | Specific RM absorbance | Specific absorbance in the reflectance mode |
| $A_{Rb}(\lambda_{1R})$ | Relative contribution of anthocyanins (b) to the specific RM absorbance at λ_{1R} | Specific TM absorbance | Specific absorbance in the transmittance mode |
| $A_{Tb}(\lambda_{1T})$ | Relative contribution of anthocyanins (b) to the specific TM absorbance at λ_{1T} | $T_m(\lambda)$ | Measured leaf diffusive transmittance at λ |
| $\varepsilon_{Rb}(\lambda), \varepsilon_{Rc}(\lambda)$ | Mean molar absorption coefficients of anthocyanins (b) or chlorophyll (c) along the reflection (R) pathway at λ , respectively | x_T, x_R | A beam trajectory in the transmittance (T) or reflectance (R) mode, respectively |
| $\varepsilon_{Tb}(\lambda), \varepsilon_{Tc}(\lambda)$ | Mean molar absorption coefficients of anthocyanins (b) or chlorophyll (c) along the transverse (T) pathway at λ , respectively | Upper left index B Upper left index D | Abaxial side Adaxial side |
| h | Leaf thickness | | |
| $I_0(\lambda)$ | Intensity of the incident light at λ | | |
| $I'_0(\lambda)$ | Intensity of light entering the leaf at λ | | |
| $I_R(\lambda)$ | Intensity of light reflected (R) from the leaf at λ | | |
| $I_{Re}(\lambda), I_{Ri}(\lambda)$ | Intensity of light reflected (R) from the leaf surface at λ (external reflection) or from internal leaf structures at λ (internal reflection), respectively | | |
| $I_T(\lambda)$ | Intensity of light transmitted (T) through the leaf at λ | | |
| K | $NDVI$ correction factor | | |

Introduction

Leaf chlorophyll content is an important physiological parameter serving as an indicator of plant stress (e.g., salt stress; Atlasi Pak et al. 2009), senescence (e.g., Hörtensteiner 2006), and nutritional status (especially nitrogen content; e.g., Loh et al. 2002). The chlorophyll content in leaves is commonly measured analytically. However, in some cases the analytical estimation is not feasible due to its invasiveness or time demands (particularly in a case of large amount of samples). Therefore, a number of portable and handheld devices (chlorophyll meters) estimating the rough chlorophyll content non-destructively are widely used nowadays.

The chlorophyll meters can be sorted out into two groups according to their principle of measurement. One group measures the leaf transmittance and the second one the leaf reflectance at selected wavelengths. An example of a chlorophyll meter measuring the leaf transmittance is a SPAD-502DL chlorophyll meter (Konica Minolta Sensing,

Osaka, Japan) showing a relative chlorophyll content in dimensionless SPAD units. The SPAD-502DL chlorophyll meter detects the light emitted by two light emitting diodes at $\lambda_{1T} = 650$ nm and $\lambda_{2T} = 940$ nm (approximate half-width of the emission spectrum is 15 and 50 nm, respectively) and transmitted through the leaf. The SPAD units are proportional to the chlorophyll *a+b* content (e.g., Coste et al. 2010; Jifon et al. 2005; Loh et al. 2002). For SPAD unit definition see “Theory” section (Eq. 10).

One representative of the second type of chlorophyll meters which measure the leaf reflectance is a Plant Pen model NDVI-300 (PSI, Brno, Czech Republic) estimating normalized difference vegetation index (NDVI, see “Theory” section, Eq. 24). The Plant Pen model NDVI-300 (Plant Pen) measurement is based on detection of light of $\lambda_{1R} = 660$ nm and $\lambda_{2R} = 740$ nm reflected by the measured leaf. It should be mentioned that this type of reflectance is of a directed character and differs from that of diffusive character measured by an integrating sphere (see further). The angles of incidence and reflectance are determined by the construction of the instrument. NDVI and other reflectance-based indexes are of high importance nowadays because of their use in remote sensing or precision agriculture (e.g., Gitelson et al. 2012).

The measurement of chlorophyll content by SPAD-502DL or Plant Pen NDVI-300 chlorophyll meters can be pronouncedly affected by various optical effects in leaves. It has been already reported, for instance, that chloroplast movement can affect the SPAD reading (Nauš et al. 2010). Moreover, the measured transmittance or reflectance can be distorted by the light scattering, inner reflectance, and sieve effect. In addition, certain leaf pigments [different from chlorophylls, e.g., anthocyanins (ACN)] absorbing in the red region could also distort the SPAD-502DL or Plant Pen reading. The ACN are red, purple, and blue-colored water-soluble pigments accumulating typically in juvenile and senescing leaves (Chalker-Scott 1999; Close and Beadle 2003; Feild et al. 2001; Hoch et al. 2001). Accumulation of ACN occurs under stress conditions such as high intensity of light (Albert et al. 2009), UV irradiance (Guo and Wang 2010; Mendez et al. 1999), extreme temperatures (e.g., Leyva et al. 1995), and under some other stresses (Chalker-Scott 1999; Merzlyak et al. 2008).

The ACN are synthesized in the cytosol and then transported to vacuoles (Tanaka et al. 2008). The distribution of ACN in leaves depends on plant species. The ACN are mainly present in the vacuoles of cell on the adaxial leaf side, predominantly in the outer epidermal layers. The ACN can also occur in palisade parenchyma (Merzlyak et al. 2008). The ACN function in leaves is believed to be the absorption of excessive solar radiation that prevents photosynthetic apparatus from photoinhibition and photodamage (Chalker-Scott 1999; Solovchenko

and Chivkunova 2011). Moreover, ACN may act as potential antioxidants (e.g., Kytridis and Manetas 2006).

Composition and content of ACN in leaves affects their resulting coloration. The ACN content in leaf can be estimated spectrophotometrically by measuring the absorbance of ACN extract. The position of ACN absorption peak depends on the used solvent and its pH (e.g., Giusti and Wrolstad 2001; Qin et al. 2010). However, in most cases, the position of this peak is between 520 and 550 nm (e.g., Gauche et al. 2010; Giusti and Wrolstad 2001; Pietrini et al. 2002; Qin et al. 2010; Sims and Gamon 2002). Above 600 nm ACN absorbance was found to be negligible (e.g., Junka et al. 2012; Karageorgou and Manetas 2006; Qin et al. 2010). Thus, the absorption spectrum of ACN and chlorophylls in vitro do not overlap above 600 nm. However, a maximum of ACN absorption in vivo was reported to be shifted toward the red region compared with the corresponding maxima in acidic alcohol extracts (Gitelson et al. 2001; Merzlyak et al. 2008). The red shift of spectrum in vivo can cause a non-zero ACN absorption even in the red region (above 600 nm; e.g., Merzlyak et al. 2008). It means that ACN can increase the leaf absorption in that wavelength region, where the chlorophylls absorb (e.g., Merzlyak et al. 2008). Consequently, the reading of chlorophyll content by SPAD-502DL or Plant Pen NDVI-300 chlorophyll meters can be affected by ACN presence in leaf.

The aim of our work was to determine the contribution of ACN to the leaf transmittance or reflectance within spectral regions which are used for estimation of the chlorophyll content by SPAD-502DL or Plant Pen NDVI-300 pocket chlorophyll meters and to suggest a correction procedure of their readings.

Theory

Concept of “specific absorbance” and correction of SPAD value

The aim of this theoretical part is to explain the computational approach for estimation of the contribution of ACN to the signal of chlorophyll meters using both transmittance and reflectance measurement. Although the principles of measurements are different, for the sake of mathematical evaluation the approach can be similar. The situation in measuring the chlorophyll-related signal is depicted in Fig. 1a. Incident light with intensity $I_0(\lambda)$ is partly reflected by leaf surface with intensity $I_{Re}(\lambda)$ and partly enters the leaf ($I'_0(\lambda)$ is the intensity of light entering the leaf at λ). Intensity $I_{Re}(\lambda)$ is $I_{Re}(\lambda) = I_0(\lambda)R_e(\lambda)$, where $R_e(\lambda)$ is the external (surface) reflectance of the leaf at λ . $R_e(\lambda)$ is

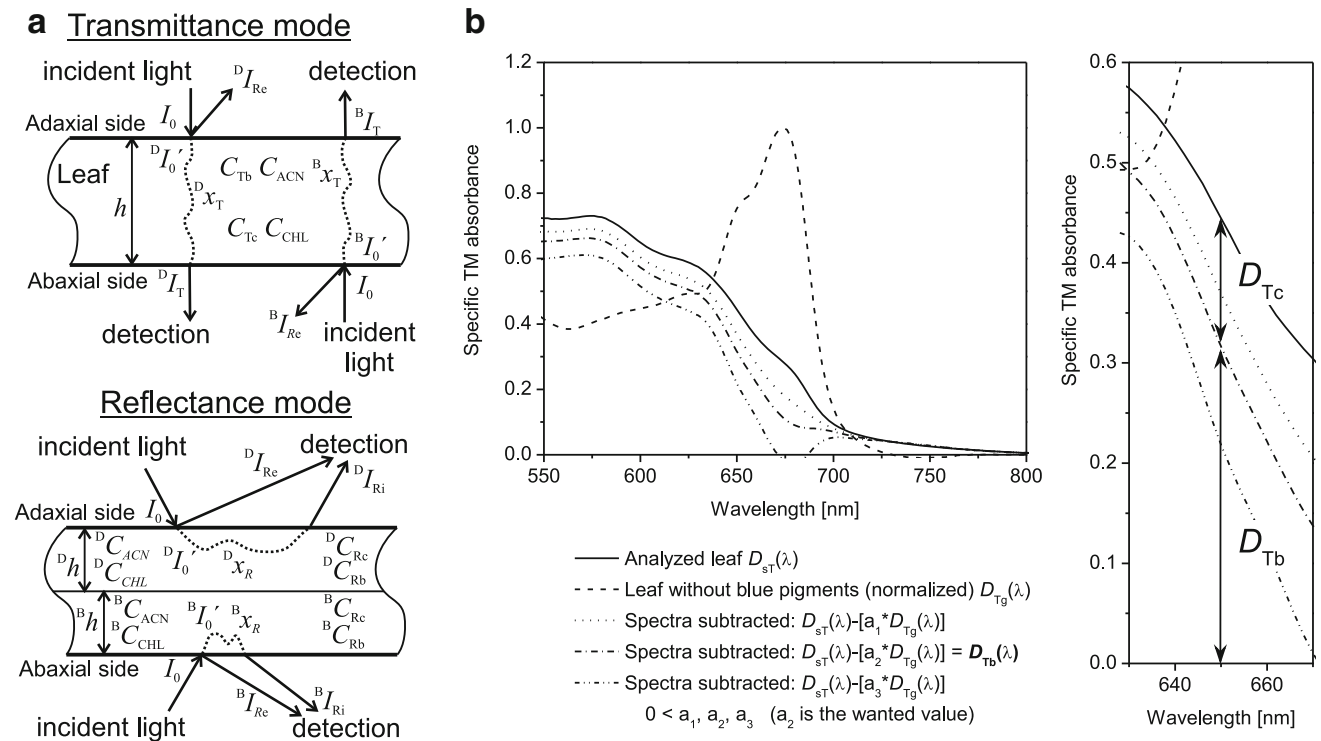


Fig. 1 a A scheme of the light beam path within a leaf in the transmittance mode (TM) or reflectance mode (RM) and the meaning of some parameters used in “Theory” section. **b** A scheme describing the procedure of the spectral subtraction. The spectra resulting from a subtraction of weighted (weighting coefficient a) normalized specific TM absorbance of a leaf without anthocyanins [$a \cdot D_{Tg}(\lambda)$] from the

specific TM absorbance of the leaf $D_{sT}(\lambda)$ are shown. When the best value of the parameter a (a_2 in this case) is found, the obtained spectrum [$(D_{sT}(\lambda) - a_2 \cdot D_{Tg}(\lambda))$] is expected to correspond to a hypothetical leaf containing only anthocyanins $D_{Tb}(\lambda)$. The spectrum of a hypothetical sample without anthocyanins $D_{Tc}(\lambda)$ is calculated as $D_{sT}(\lambda) - D_{Tb}(\lambda)$ (see the detail in the right part)

governed mostly by the Fresnel’s equations. If we expect that cuticle and cell walls of surface cell layer(s) contain no pigments, this reflection should be independent on chlorophyll and ACN pigment content.

After entering the leaf, the light passes a beam trajectory x_T in the transmittance mode. In the spectral region of our interest (above 600 nm) we suppose that only chlorophylls (a and b) and ACN absorb. So we neglect the contribution of carotenoids, and even phytochromes or chlorophyll precursors or degradation products.

If we assume a validity of the Lambert–Beer’s law in form:

$$I_T(\lambda) = I'_0(\lambda) \cdot 10^{-D_T(\lambda)} = I_0(\lambda)(1 - R_e(\lambda)) \cdot 10^{-D_T(\lambda)}, \quad (1)$$

where $I_T(\lambda)$ is the intensity of light transmitted through the leaf at λ , then the overall optical density (here named as “specific absorbance”) at wavelength λ in the case of transmittance mode (in short: overall specific TM absorbance at λ) is:

$$D_T(\lambda) = D_{Tc}(\lambda) + D_{Tb}(\lambda) + D_{Tr}(\lambda) = \varepsilon_{Tc}(\lambda)C_{Tc}x_T + \varepsilon_{Tb}(\lambda)C_{Tb}x_T + b_T(\lambda)x_T, \quad (2)$$

where D_{Tc} is specific TM absorbance of chlorophyll at λ , D_{Tb} is specific TM absorbance of ACN at λ , $\varepsilon_{Tc}(\lambda)$ and $\varepsilon_{Tb}(\lambda)$ are the mean molar absorption coefficients of chlorophyll and ACN, respectively, along the transverse pathway x_T in the leaf at λ , and C_{Tc} and C_{Tb} are the mean theoretical chlorophyll and ACN concentrations [with unit ($\text{mol l}^{-1} = \text{M}$)], respectively, in the leaf. We use here the abbreviation ACN and the name anthocyanins for all possible blue pigments (see lower index b) absorbing in vivo above 600 nm (even though primarily for anthocyanins). As part of light on the transverse pathway can be lost for detection independently on the presence of pigments due to a complex of optical phenomena (reflection, scatter, refraction, and diffraction), the third part of the sum in Eq. 2 expresses a contribution of these effects to the overall specific TM absorbance at λ . Here, $D_{Tr}(\lambda)$ is specific TM absorbance caused by reflection, scatter, refraction, and diffraction at λ , the function $b_T(\lambda)$ expresses the mentioned effects.

When inserting Eq. 2 to Eq. 1 and designating $10^{-b_T(\lambda)x_T} = \tau(\lambda)$, the Lambert–Beer’s law can be rewritten to the following form:

$$I_T(\lambda) = I_0(\lambda)(1 - R_e(\lambda)) \cdot 10^{-[D_{Tc}(\lambda)+D_{Tb}(\lambda)]} \cdot \tau(\lambda). \tag{3}$$

The measured leaf diffusive transmittance at λ [when substituting Eq. 3 for $I_T(\lambda)$] is:

$$T_m(\lambda) = \frac{I_T(\lambda)}{I_0(\lambda)} = (1 - R_e(\lambda))\tau(\lambda) \cdot 10^{-[\varepsilon_{Tc}(\lambda)C_{Tc} + \varepsilon_{Tb}(\lambda)C_{Tb}]x_T}. \tag{4}$$

If we suppose for simplicity that $b_T(\lambda)$ and $R_e(\lambda)$ are wavelength-independent (at least in the red and near infrared region), then $(1 - R_e)\tau$ can be obtained at those wavelengths λ_{2T} where $\varepsilon_{Tc}(\lambda_{2T}) = \varepsilon_{Tb}(\lambda_{2T}) = 0$, i.e., in the near infrared region where absorption of both pigments is null. Substituting these zero values to exponent of Eq. 4, we get:

$$T_m(\lambda_{2T}) = (1 - R_e)\tau \tag{5}$$

Thus, the desired factor $(1 - R_e)\tau$ is equal to the measured leaf diffusive transmittance in the infrared region. Result of Eq. 5 can be inserted to Eq. 4, and Eq. 4 can be rewritten to:

$$T_m(\lambda) = T_m(\lambda_{2T}) \cdot 10^{-[\varepsilon_{Tc}(\lambda)C_{Tc} + \varepsilon_{Tb}(\lambda)C_{Tb}]x_T} \tag{6}$$

Decimal logarithm of both sides of Eq. 6 leads to the following form:

$$\begin{aligned} \log T_m(\lambda_{2T}) - \log T_m(\lambda) &= [\varepsilon_{Tc}(\lambda)C_{Tc} + \varepsilon_{Tb}(\lambda)C_{Tb}]x_T \\ &= D_{Tc}(\lambda) + D_{Tb}(\lambda) = D_{sT}(\lambda) \end{aligned} \tag{7}$$

where $D_{sT}(\lambda)$ is calculated specific TM absorbance at λ . Equation 7 can be read in a way that it is possible to calculate $D_{sT}(\lambda)$ spectrum from spectrum of $T_m(\lambda)$. Furthermore, according to Eq. 7, spectrum of $D_{sT}(\lambda)$ is given as a sum of spectra of specific TM absorbance of chlorophyll and of ACN at λ .

Since the external reflectance of the leaf R_e is different for the adaxial and abaxial leaf sides (see, e.g., McClendon and Fukshansky 1990) the quantity $D_{sT}(\lambda)$ will be slightly different for the two leaf sides. This is reflected in slightly different values of $T_m(\lambda_{2T})$ measured from different leaf sides (for selected leaves shown in Fig. 2a see Fig. 2b). So we should distinguish between ${}^D D_{sT}(\lambda)$ calculated for the adaxial (left upper index D) leaf side:

$$\begin{aligned} {}^D D_{sT}(\lambda) &= {}^D D_{Tc}(\lambda) + {}^D D_{Tb}(\lambda) = [{}^D \varepsilon_{Tc}(\lambda)C_{Tc} + {}^D \varepsilon_{Tb}(\lambda)C_{Tb}]x_T \\ &= \log {}^D T_m(\lambda_{2T}) - \log {}^D T_m(\lambda) \end{aligned} \tag{8}$$

and ${}^B D_{sT}(\lambda)$ calculated for the abaxial leaf side (left upper index B instead of D). It is supposed here that C_{Tc} (C_{Tb} , respectively) is the same for calculation of ${}^D D_{sT}(\lambda)$ and ${}^B D_{sT}(\lambda)$.

The different spectra ${}^D T_m(\lambda)$ and ${}^B T_m(\lambda)$ are the base for the concept of transmittance spectral polarity of leaves.

The result of comparison of the measured transmittances in the region of λ_{2T} (no absorption of pigments; Fig. 2b) is that the transmittance measured from the abaxial leaf side was in all cases higher than that one measured from the adaxial leaf side. The ratio (drawing from Eq. 5):

$$\frac{{}^B T_m(\lambda_{2T})}{{}^D T_m(\lambda_{2T})} = \frac{{}^B \tau(\lambda_{2T})}{{}^D \tau(\lambda_{2T})} \cdot \frac{(1 - {}^B R_e)}{(1 - {}^D R_e)} \tag{9}$$

is governed mostly by the relation $\frac{{}^B \tau(\lambda_{2T})}{{}^D \tau(\lambda_{2T})}$ which is higher than 1. This corresponds to lower values of the coefficient of light inner scatter and reflection in case of passing in the direction from abaxial to the adaxial leaf side. The higher transmittance from the abaxial leaf side cannot be explained by difference in the external reflection. It has been shown (e.g., McClendon and Fukshansky 1990) that the external (surface) reflection is higher in case of the abaxial (about 8 %) than adaxial (about 4 %) leaf side. This is an opposite tendency than in Fig. 2b.

The definition and evaluation of the SPAD values are corresponding to Eq. 7:

$$\begin{aligned} SPAD &= l \cdot \left[\log \frac{I_T(\lambda_{2T})}{I_0(\lambda_{2T})} - \log \frac{I_T(\lambda_{1T})}{I_0(\lambda_{1T})} \right] \\ &= l \cdot [\log T_m(\lambda_{2T}) - \log T_m(\lambda_{1T})] \\ &= l \cdot [\log T_m(940 \text{ nm}) - \log T_m(650 \text{ nm})] \\ &= l \cdot D_{sT}(650 \text{ nm}), \end{aligned} \tag{10}$$

where l is a confidential proportionality coefficient which defines the relative SPAD units (e.g., Nauš et al. 2010). Equation 10 is written in the form of calculated specific TM absorbance at λ defined above (Eq. 7). The SPAD values measured for adaxial (left upper index D) and abaxial (index B) side of leaf should be distinguished.

Getting back to Eq. 7 (Eq. 8, respectively): since the spectrum of $D_{sT}(\lambda)$ is composed of the spectra $D_{Tc}(\lambda)$ and $D_{Tb}(\lambda)$, it should be possible, by contrast, to decompose $D_{sT}(\lambda)$ to two single spectra: $D_{Tc}(\lambda)$ and $D_{Tb}(\lambda)$ (we propose the method how to do it based on spectral subtraction, see below). Obtained spectrum $D_{Tb}(\lambda)$ can be used to compute the relative contribution of ACN to the specific TM absorbance at λ_{1T} . For adaxial side of leaf (analogically for abaxial side of leaf; left upper index B), this quantity is:

$${}^D \Delta_{Tb}(\lambda_{1T}) = \frac{{}^D D_{Tb}(\lambda_{1T})}{{}^D D_{Tc}(\lambda_{1T}) + {}^D D_{Tb}(\lambda_{1T})} \tag{11}$$

After obtaining the quantity ${}^D \Delta_{Tb}(\lambda_{1T})$, the relative contribution of ACN to the SPAD signal for adaxial side (${}^D \Delta_b({}^D SPAD)$) can be evaluated according to the following expression:

$${}^D \Delta_b({}^D SPAD) = {}^D \Delta_{Tb}(\lambda_{1T}), \tag{12}$$

analogically for abaxial side (left upper index B). The relative contribution of ACN to the SPAD signal expressed

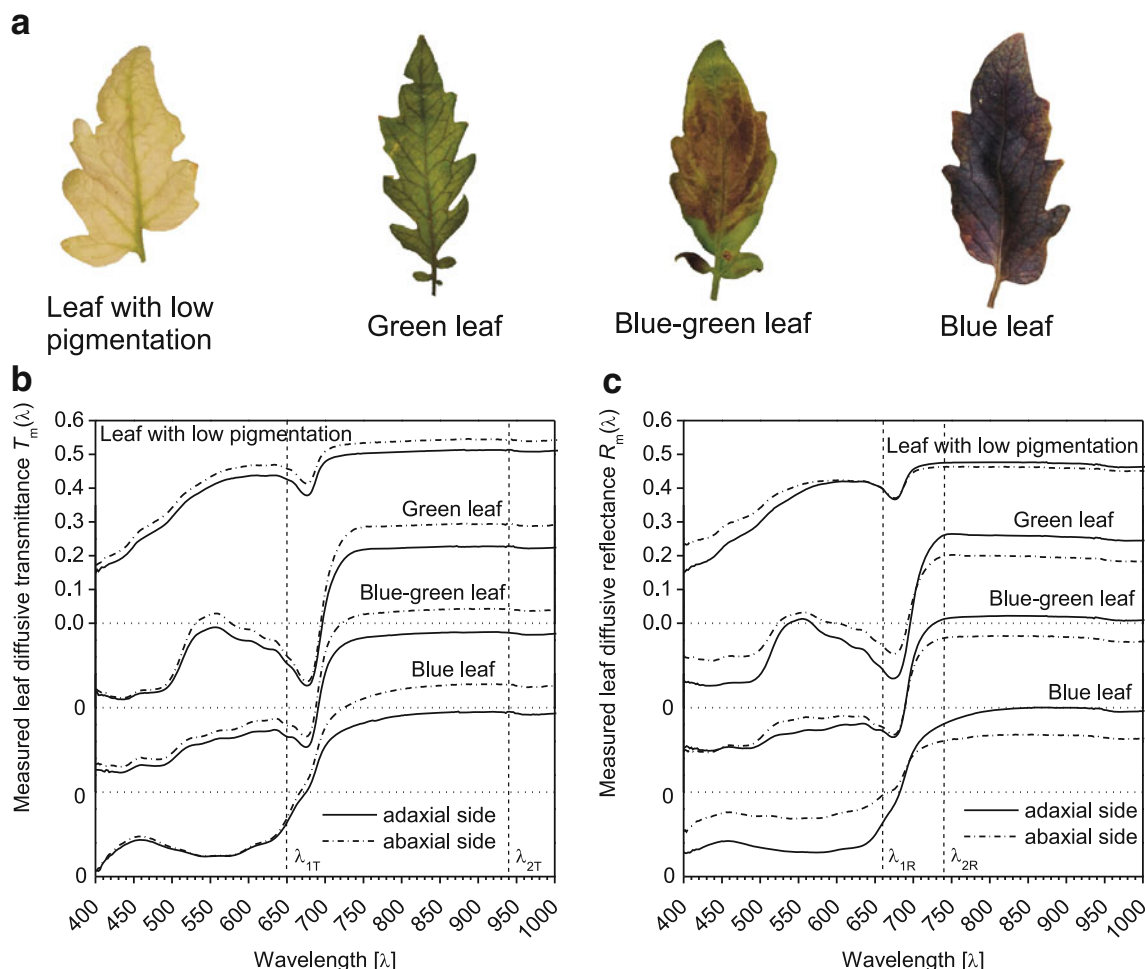


Fig. 2 **a** Photos of four selected typical leaves with different colors: leaf with low pigmentation (pale yellow-green color), green leaf, blue-green leaf, and blue leaf. **b** Spectra of the measured leaf diffusive transmittance from the adaxial leaf side (solid line) and from the abaxial leaf side (dash-dotted line) corresponding to the selected leaves (measured by LI-1800-12). The wavelengths of SPAD

detection (λ_{1T} , λ_{2T} ; dashed vertical lines) are marked. **c** Spectra of the measured leaf diffusive reflectance from the adaxial leaf side (solid line) and from the abaxial leaf side (dash-dotted line) corresponding to the selected leaves (measured by LI-1800-12). The wavelengths of NDVI detection (λ_{1R} , λ_{2R} ; dashed vertical lines) are marked

in per cents is ${}^D\Delta_{Tb}(\lambda_{1T}) \cdot 100$. Equation 12 follows from the definition and evaluation of the SPAD values (Eq. 10).

The corrected value of SPAD reading proportional only to the chlorophyll content ($SPAD_C$) would be for adaxial side (for abaxial analogically; index B):

$${}^D SPAD_C = {}^D SPAD \cdot [1 - {}^D\Delta_{Tb}(\lambda_{1T})]. \tag{13}$$

Reflectance and NDVI correction

Quite a similar approach may be used for the reflectance measurements (Fig. 1a) although little different conclusions will be drawn. In this case the situation at the adaxial leaf side may be more distinctly different from that at the abaxial side. We recall here that the measured leaf diffusive reflectance at λ [$R_m(\lambda)$] can be understood as composed of the external (surface) reflectance of the leaf at λ

[$R_e(\lambda)$] and internal reflectance of the leaf at λ [$R_i(\lambda)$] (see e.g., McClendon and Fukshansky 1990): $R_m(\lambda) = R_e(\lambda) + R_i(\lambda)$. The internal reflectance of the leaf at λ represents that part of incident light entering the interior of the leaf and returning back to the space above the leaf. We expect this part to reflect the presence of mentioned pigments in reflectance mode.

Inside the leaf, the beam trajectory in the reflectance mode is designated as x_R (Fig. 1a). The measured leaf diffusive reflectance R_m is:

$$R_m(\lambda) = \frac{I_R(\lambda)}{I_0(\lambda)}, \tag{14}$$

where $I_R(\lambda)$ is intensity of the light reflected from the leaf at λ . However, now:

$$I_R(\lambda) = I_{Re}(\lambda) + I_{Ri}(\lambda), \tag{15}$$

where $I_{Ri}(\lambda)$ is intensity of the light reflected from internal leaf structures at λ .

In order to simplify the model we suppose that both green (chlorophylls) and blue pigments (mainly ACN) influence only the internal reflectance $R_i(\lambda)$. Moreover, we expect the R_e to be independent on wavelength. Similarly to Eq. 1, for reflectance mode (RM), it holds Lambert–Beer’s law:

$$I_{Ri}(\lambda) = I_0(\lambda)(1 - R_e) \cdot 10^{-D_R(\lambda)}. \tag{16}$$

In analogy with the transmittance mode, the parameter $D_R(\lambda)$ from Eq. 16 is overall specific RM absorbance at λ and can be expressed as:

$$D_R(\lambda) = D_{Rc}(\lambda) + D_{Rb}(\lambda) + D_{Rr}(\lambda) = \varepsilon_{Rc}(\lambda)C_{Rc}x_R + \varepsilon_{Rb}(\lambda)C_{Rb}x_R + b_R(\lambda)x_R, \tag{17}$$

where D_{Rc} is specific RM absorbance of chlorophyll at λ , D_{Rb} is specific RM absorbance of ACN at λ , $\varepsilon_{Rc}(\lambda)$ and $\varepsilon_{Rb}(\lambda)$ are the mean molar absorption coefficients of chlorophyll and ACN, respectively, along the reflection pathway x_R in the leaf at λ , and C_{Rc} and C_{Rb} are the mean theoretical chlorophyll and ACN, respectively, concentrations along the reflection pathway in the leaf. $D_{Rr}(\lambda)$ is specific RM absorbance caused by reflection, scatter, refraction, and diffraction at λ .

When inserting Eq. 17 to Eq. 16 and designating $10^{-b_R(\lambda)x_R} = \rho(\lambda)$, the Lambert–Beer’s law can be rewritten to following form:

$$I_{Ri}(\lambda) = I_0(\lambda)(1 - R_e) \cdot 10^{-[\varepsilon_{Rc}(\lambda)C_{Rc} + \varepsilon_{Rb}(\lambda)C_{Rb}]x_R} \cdot \rho(\lambda) \tag{18}$$

and therefore:

$$I_R(\lambda) = I_{Re}(\lambda) + I_{Ri}(\lambda) = I_0(\lambda)[R_e + (1 - R_e) \cdot 10^{-[\varepsilon_{Rc}(\lambda)C_{Rc} + \varepsilon_{Rb}(\lambda)C_{Rb}]x_R} \cdot \rho(\lambda)] \tag{19}$$

Expressing the measured leaf diffusive reflectance (inserting Eq. 19 to Eq. 14) we obtain:

$$R_m(\lambda) = \frac{I_R(\lambda)}{I_0(\lambda)} = R_e + (1 - R_e) \cdot 10^{-[\varepsilon_{Rc}(\lambda)C_{Rc} + \varepsilon_{Rb}(\lambda)C_{Rb}]x_R} \cdot \rho(\lambda). \tag{20}$$

To simplify the approach, we assume that $\rho(\lambda)$ is independent on λ . In the region of λ_{2R} where the pigment absorption is null ($\varepsilon_{Rc}(\lambda_{2R}) = \varepsilon_{Rb}(\lambda_{2R}) = 0$), it holds:

$$R_m(\lambda_{2R}) = \frac{I_R(\lambda_{2R})}{I_0(\lambda_{2R})} = R_e + (1 - R_e)\rho. \tag{21}$$

If expressing $(1 - R_e)\rho$ from Eq. 21 and replace it in Eq. 20, we obtain:

$$R_m(\lambda) = R_e + [R_m(\lambda_{2R}) - R_e] \cdot 10^{-[\varepsilon_{Rc}(\lambda)C_{Rc} + \varepsilon_{Rb}(\lambda)C_{Rb}]x_R}. \tag{22}$$

In reflectance mode, the spectrum of measured leaf diffusive reflectance and the external reflectance R_e for the adaxial side of leaf differ from that of abaxial side. In following, we focus on adaxial side (left upper index D; for simplicity, some equations are without indexes), the abaxial one is analogical (with left upper index B). The different designations, although seems too complicated, are necessary because in many cases, mostly in bifacial leaves, there is a distinct difference in pigments concentrations and absorption properties at different sides of the leaf. Theoretically, the beam trajectory in the reflectance mode at the adaxial leaf side ${}^D x_R$ may be different from that at the abaxial side ${}^B x_R$ (e.g., Terashima and Saeki 1983).

Decimal logarithm of both sides of Eq. 22 leads to following form:

$$\begin{aligned} \log \left[\frac{{}^D R_m(\lambda_{2R}) - {}^D R_e}{1 - {}^D R_e} \right] - \log \left[\frac{{}^D R_m(\lambda) - {}^D R_e}{1 - {}^D R_e} \right] &= \left[{}^D \varepsilon_{Rc}(\lambda) {}^D C_{Rc} + {}^D \varepsilon_{Rb}(\lambda) {}^D C_{Rb} \right] {}^D x_R \\ &= {}^D D_{Rc}(\lambda) + {}^D D_{Rb}(\lambda) = {}^D D_{sR}(\lambda), \end{aligned} \tag{23}$$

where ${}^D D_{sR}(\lambda)$ is the calculated specific RM absorbance at λ . Equation 23 can be read in way that it is possible to calculate ${}^D D_{sR}(\lambda)$ spectrum from spectrum of $R_m(\lambda)$ and from R_e . So in case of the reflection measurements as compared to the transmittance measurements (see Eq. 7), the effect of external reflection is not canceled and should be taken into account in the evaluations (we propose the method how to find out the value of R_e , see below).

The NDVI is defined as:

$$NDVI = \frac{R_m(\lambda_{IR}) - R_m(\lambda_R)}{R_m(\lambda_{IR}) + R_m(\lambda_R)} = \frac{R_m(\lambda_{2R}) - R_m(\lambda_{1R})}{R_m(\lambda_{2R}) + R_m(\lambda_{1R})}, \tag{24}$$

where λ_R is the wavelength in the red region and λ_{IR} is the wavelength in the near infrared region. The measured leaf diffusive reflectance appears in Eq. 24, however, the portable instruments use more often the reflectance of directed character.

Inserting the $R_m(\lambda)$ from Eqs. 22 to 24, we get the NDVI definition in form of specific absorbances [we suppose that $\varepsilon_{Rc}(\lambda_{2R}) = \varepsilon_{Rb}(\lambda_{2R}) = 0$]:

$$NDVI = \frac{[R_m(\lambda_{2R}) - R_e][1 - 10^{-D_{sR}(\lambda_{1R})}]}{2R_e + [R_m(\lambda_{2R}) - R_e][1 + 10^{-D_{sR}(\lambda_{1R})}]}. \tag{25}$$

Similar to $D_{sT}(\lambda)$, it should be possible to decompose ${}^D D_{sR}(\lambda)$ into two single spectra: ${}^D D_{Rc}(\lambda)$ and ${}^D D_{Rb}(\lambda)$. The spectrum ${}^D D_{Rb}(\lambda)$ can be used to compute the relative contribution of ACN to the specific RM absorbance at λ_{1R} . For the adaxial side of leaf, this quantity is:

$${}^D\Delta_{Rb}(\lambda_{1R}) = \frac{{}^D D_{Rb}(\lambda_{1R})}{{}^D D_{Rc}(\lambda_{1R}) + {}^D D_{Rb}(\lambda_{1R})}. \tag{26}$$

The correction of the NDVI value for the ACN contribution is more complex. As SPAD is proportional to $D_{sT}(\lambda_{1T})$ (see Eq. 10), NDVI is also proportional to $D_{sR}(\lambda_{1R})$ (Eq. 25). Therefore, the same principle of correction (see Eq. 13 for SPAD) can be used: $D_{sR}(\lambda_{1R})$ in Eq. 25 is multiplied by factor $[1 - {}^D\Delta_{Rb}(\lambda_{1R})]$. The corresponding corrected NDVI value expressing only the signal caused by chlorophylls is:

$$\begin{aligned} NDVI_C &= \frac{[R_m(\lambda_{2R}) - R_e][1 - 10^{-D_{sR}(\lambda_{1R})[1 - \Delta_{Rb}(\lambda_{1R})]}]}{2R_e + [R_m(\lambda_{2R}) - R_e][1 + 10^{-D_{sR}(\lambda_{1R})[1 - \Delta_{Rb}(\lambda_{1R})]}]} \\ &= \frac{[R_m(\lambda_{2R}) - R_e][1 - K \cdot 10^{-D_{sR}(\lambda_{1R})}]}{2R_e + [R_m(\lambda_{2R}) - R_e][1 + K \cdot 10^{-D_{sR}(\lambda_{1R})}]}, \end{aligned} \tag{27}$$

where K is the NDVI correction factor:

$$K = 10^{\Delta_{Rb}(\lambda_{1R}) \cdot D_{sR}(\lambda_{1R})}. \tag{28}$$

In the case that R_e is not considered ($R_e = 0$), Eq. 27 can be rewritten to:

$$NDVI_C = \frac{1 - K \cdot 10^{-D_{sR}(\lambda_{1R})}}{1 + K \cdot 10^{-D_{sR}(\lambda_{1R})}} \tag{29}$$

Using Eqs. 29 and 25 (with $R_e = 0$) we can obtain:

$$NDVI_C = \frac{NDVI(1 + K) + 1 - K}{NDVI(1 - K) + 1 + K} \tag{30}$$

We have tested the difference between results obtained with Eq. 30 (without consideration of external reflection) and by Eq. 27 including R_e . It appears that the omission of external reflection may lead to overestimation of the NDVI signal up to 10 % in case of adaxial leaf side and up to 20 % for abaxial side. Some authors may look for only relative changes and then the omission of R_e may not cause large mistakes and Eq. 30 may suffice. In following parts we use the approach without consideration of R_e .

Estimation of the external (surface) reflectance R_e

An experimental procedure for the estimation of R_e has been published by McClendon and Fukshansky (1990). This procedure was not suitable for our purposes, since there was an insufficient amount of homogeneous material.

The analysis of the leaf transmittance and reflectance spectra in the near infrared region shows that these spectra are not suitable for the R_e estimation. The basic behavior of the spectra in this spectral region is unexpected and seemingly in contradiction to logics of the phenomenon. For instance, the R_e is known to be higher at the abaxial side of the leaf (e.g., McClendon and Fukshansky 1990),

however, also the transmittance is higher (see Fig. 2b). We have an explanation for this effect but this is not the main goal of this paper and will be published elsewhere.

To estimate R_e it has been found necessary to use the spectra in the visible region (400–750 nm). We have shown that the external reflectance R_e is not reflected in the expression for specific absorbance in the transmittance mode $D_{sT}(\lambda)$ (Eq. 7). So this expression may be taken as basic for the calculation of R_e to correct the reflectance spectra.

The main idea of the procedure is a supposition that the shape of the specific absorbance spectra is the same in both transmittance and reflectance mode of detection. This means we expect the spectra to have the same shape across the leaf and at both sides. This supposition may be fulfilled, at least to high level, only in leaves not containing blue pigments. The leaves containing blue pigments are strongly polar and our supposition cannot be fulfilled. Although there is certain polarity in green leaves too (e.g., in the content of chlorophyll *b* and long-wavelength spectral forms of chlorophyll *a*), we expect this effect to be negligible if wavelengths of predominant chlorophyll *a* absorption are chosen.

A simplest approach to compare the shape of two spectra is to choose two suitable wavelengths and to calculate the ratio of specific absorbances at these two wavelengths. In case of similarity this ratio should be the same in both compared spectra. We have chosen the wavelengths in the red chlorophyll *a* maximum (around 670 nm), in the green minimum (around 550 nm), and blue maximum (around 430 nm). The ratio of specific absorbances at these wavelengths in the transmittance mode is:

$$P_T = \frac{D_{sT}(\lambda_1)}{D_{sT}(\lambda_2)} = \frac{\log \frac{T_m(\lambda_{2T})}{T_m(\lambda_1)}}{\log \frac{T_m(\lambda_{2T})}{T_m(\lambda_2)}}. \tag{31}$$

In the reflectance mode, the expression for the band ratio is more complicated:

$$P_R = \frac{D_{sR}(\lambda_1)}{D_{sR}(\lambda_2)} = \frac{\log \left[\frac{R_m(\lambda_{2R}) - R_e}{R_m(\lambda_1) - R_e} \right]}{\log \left[\frac{R_m(\lambda_{2R}) - R_e}{R_m(\lambda_2) - R_e} \right]}. \tag{32}$$

If we expect the same shape of the spectra, it must hold: $P_T = P_R$.

Because the value of P_T is known, we fit the R_e value in the P_R expression to find the P_R value to be equal to P_T with the demanded minimal difference (several %). We have found R_e to be 6.82 ± 0.30 % (mean \pm standard deviation) for the abaxial leaf side and 4.59 ± 0.33 % for the adaxial leaf side. These two values have been used to correct the reflectance spectra for the external reflectance.

Specific absorbance spectral subtraction

The quantity ${}^D\Delta_{Tb}(\lambda_{1T})$ can be calculated from ${}^D D_{Tb}(\lambda_{1T})$ and ${}^D D_{Tc}(\lambda_{1T})$ obtained by the following procedure: in the spectral region 550–800 nm, the spectrum of the mean normalized specific TM absorbance of a leaf without ACN at λ for the adaxial leaf side (${}^D D_{Tg}(\lambda)$) multiplied by a constant number ($a > 0$) was subtracted from the spectrum of the corresponding calculated specific absorbance (${}^D D_{sT}(\lambda)$) of the analyzed leaf. The value of the constant number a has to be found so that the spectrum resulting from the subtraction (i.e., ${}^D D_{sT}(\lambda) - a \cdot {}^D D_{Tg}(\lambda)$) reveals no distinct band pertaining to chlorophylls.

The value of number a was selected maximal possible so that the values of ${}^D D_{sT}(\lambda) - a \cdot {}^D D_{Tg}(\lambda)$ were positive in the spectral region 550–800 nm and there was no inflection point in the spectral region 680–690 nm at the same time (one or two inflection points appear on the subtracted curve in case of uncorrected subtraction). The quantitative criterion demanded a deviation of the found value to the incorrect one to be less than 5 %.

When the a value is found, the spectrum of specific TM absorbance of ACN at λ for adaxial leaf side is ${}^D D_{Tb}(\lambda) = {}^D D_{sT}(\lambda) - a \cdot {}^D D_{Tg}(\lambda)$ and the spectrum of specific TM absorbance of chlorophylls for adaxial leaf side is ${}^D D_{Tc}(\lambda) = {}^D D_{sT}(\lambda) - {}^D D_{Tb}(\lambda)$. The scheme of the subtraction procedure is shown in Fig. 1b. The procedure has been done by hand by a series of refinement of the a value to reach a desired precision (5 %).

A similar procedure can be used for calculations of the quantities ${}^B\Delta_{Tb}(\lambda_{1T})$, ${}^B\Delta_{Rb}(\lambda_{1R})$, and ${}^B\Delta_{Rb}(\lambda_{1R})$. These quantities can be calculated from ${}^B D_{Tb}(\lambda_{1T})$, ${}^B D_{Tc}(\lambda_{1T})$, ${}^B D_{Rb}(\lambda_{1R})$, ${}^B D_{Rc}(\lambda_{1R})$ and ${}^B D_{Rb}(\lambda_{1R})$, ${}^B D_{Rc}(\lambda_{1R})$ obtained by a similar procedure as described above (the designation of other quantities is: ${}^B D_{Tg}(\lambda)$, ${}^B D_{sT}(\lambda)$, ${}^B D_{Rg}(\lambda)$, ${}^B D_{sR}(\lambda)$, ${}^B D_{Rg}(\lambda)$, ${}^B D_{sR}(\lambda)$).

Materials and methods

Tomato plants (*Solanum lycopersicum* L. cv. Rutgers) were cultivated in Olomouc, Czech Republic, from October 2010 to September 2011 and from February to June 2012. The seeds were inserted into pots filled with a seed soil substrate (Potgrond H, Klasmann Deilmann GmbH, Germany). Plants were cultivated in glasshouse under natural light conditions. The 1-month-old plants were transferred to a growth chamber SGC.170.PFX.J (Weiss-Gallenkamp Ltd., Loughborough, UK) and kept at 25 °C, relative air humidity 50 %, under 14 h light (130 $\mu\text{mol photons of photosynthetically active radiation (PAR) m}^{-2} \text{ s}^{-1}$)/8 h dark cycle with 1 h of linear light-rise and light-set. The

plants were watered regularly (once in 2 days, about 100 ml per pot). After 2 months, the plants were removed from the growth chamber and placed behind the window to allow plants growth on specific light conditions (sunlight coming through common window glass, see below). The plants growing behind the window were of long stem and smaller leaves.

The sunlight of high intensity (about 1,300 $\mu\text{mol photons of PAR m}^{-2} \text{ s}^{-1}$) coming through window glass contains a visible and UV-A part of spectrum (wavelengths above 325 nm), however, a UV-B part is absorbed by window glass (generally accepted fact, checked by the spectra measurement, data not shown). Green tomato leaves of mature plants were exposed to illumination described above for period of several weeks (about 4 h daily) till they changed their coloration to violet to blue. Plants old 10–11 and 6 months were used for measurement (most of plants passed flowering, some plants from the 6-months-old group were flowering at the time of measurement). The violet to blue coloration was observed mostly on plants at the time and after the time of flowering.

Control plants were placed to the same place, however, protected from the light condition mentioned above. Instead of sunlight filtered by window glass, the leaves of control plants were exposed to a low-intensity visible light (coming from a fluorescent tube, about 20 $\mu\text{mol photons of PAR m}^{-2} \text{ s}^{-1}$) which did not contain the UV-A part of spectrum (up to 380 nm). The leaves of control plants remained green with no indication of the blue color.

Leaves of the lowest stores bearing signs of senescence (lower chlorophyll content) with different levels of blue coloration were selected for the measurements. Neither the age of plants nor the flowering phase were of primary importance for our experiments, the only criterion for selection of the measured leaves was the color of leaves. Leaflets were detached from the plant and their petioles were immediately inserted to a tube filled with tap water to prevent leaflet desiccation. A representative part of the leaflet was enclosed in a paper mask (diameter of aperture was 14 mm) allowing an exact measurement at the same place of the leaf from both abaxial and adaxial side. The leaf part in paper mask was used to measure the SPAD and NDVI values and spectra of the leaf diffusive transmittance and diffusive reflectance (see below). The same part of leaf was finally used for an analytical estimation of the chlorophyll and ACN content.

SPAD and NDVI values measurement

A chlorophyll meter SPAD-502DL (Konica Minolta Sensing, Osaka, Japan) was used to measure SPAD values on the adaxial and abaxial leaf side in the region delimited by the paper mask. The measurement was repeated five

times in different places of the region and the mean value was calculated. Then, by a similar way, the NDVI measurement was done using a Plant Pen NDVI-300 (PSI, Brno, Czech Republic). Before the measurement, the Plant Pen was calibrated by measuring the reflectance from a white plastic reflective reference surface (delivered by a producer as a part of the instrument) without sample.

Spectra of leaf transmittance and reflectance

Spectra of the leaf diffusive transmittance and diffusive reflectance in the spectral region 380–1,100 nm were measured using a portable spectroradiometer LI-1800 (LI-COR, Lincoln, Nebraska, USA) combined with a LI-1800-12 (LI-COR, Lincoln, Nebraska, USA) integrating sphere (see e.g., Nauš et al. 2008). The spectra were measured both from the adaxial and abaxial leaf side on a part of leaf enclosed in the paper mask. Such a complete set of four spectra allowed an evaluation of the leaf absorbance detected from both leaf sides.

Analytical estimation of chlorophyll and anthocyanin contents

The disks of 14 mm diameter have been cut off from the leaf part at the site used for the measurements described above. The disks were frozen and kept at $-80\text{ }^{\circ}\text{C}$. One half of the leaf disk was homogenized in 80 % (v/v) acetone with small amount of MgCO_3 and centrifuged at room temperature (3,600g for 5 min). Chlorophyll *a+b* content in supernatant was determined spectrophotometrically (Unicam UV550, Thermo Spectronic, Cambridge, UK) according to Lichtenthaler (1987) with a spectral slit width 1 nm. The chlorophyll *a+b* content in the leaf disk estimated analytically (C_{CHL}) is expressed in $[\mu\text{g cm}^{-2}]$ or $[\text{nmol cm}^{-2}]$ (calculated by division of the values in $[\mu\text{g cm}^{-2}]$ by molecular weight of chlorophyll *a* (893.49 g mol^{-1}) and of chlorophyll *b* (906.51 g mol^{-1})).

The second half of the leaf disk was homogenized in 1 ml of cold ethanol containing 1 % (v/v) HCl and centrifuged at 12,500 g for 10 min at $4\text{ }^{\circ}\text{C}$. The common 35 % (v/v) HCl was used for the solvent preparation. The supernatant containing the dissolved ACN was collected and the pellet was resuspended in 1 ml of 1 % (v/v) HCl in ethanol and centrifuged 12,500 g for 10 min at $4\text{ }^{\circ}\text{C}$. The supernatant was again collected and added to the previously collected one. The ACN content in the overall supernatant was determined spectrophotometrically (Unicam UV550) according to Sheoran et al. (2006). The absorbances at 535 and 640 nm (A_{535} and A_{640}) of the sample were recorded and the ACN content in the leaf disk (C_{ACN}) was calculated according to the equation: $C_{\text{ACN}}[\text{nmol cm}^{-2}] = (A_{535} - 1.15A_{640}) \cdot$

$2.63 \cdot 10^{-5}$, where the used molar extinction coefficient at 535 nm for ACN was of $3.8 \cdot 10^4\text{ M}^{-1}\text{ cm}^{-1}$ (Sheoran et al. 2006).

Results and discussion

Effect of blue pigments

To explore an extent of the ACN-caused distortion of SPAD or NDVI values, we exposed senescing tomato plants to light conditions that caused strong blue to violet coloration of the senescing leaves (Fig. 2a) reflecting the ACN accumulation. The conditions leading to the change of leaf color included in our case direct solar radiation (sunlight) of high intensity ($1,300\text{ }\mu\text{mol photons of PAR m}^{-2}\text{ s}^{-1}$) and UV-A part of the spectrum (wavelengths above 325 nm).

By changing the leaf color, the spectra of leaf diffusive transmittance and reflectance changed too. The representative spectra of selected leaves (Fig. 2a) are depicted in Fig. 2b, c. The shape of the spectrum of leaf diffusive transmittance above 500 nm depends mainly on chlorophyll and ACN content. The leaves with very low pigment content evinced an increased leaf diffused transmittance in a region at about 500–700 nm compared to the spectrum of green leaf diffusive transmittance (Fig. 2b). The leaf diffusive transmittance in region at about 520–620 nm is decreasing with the increasing ACN content in the leaf (e.g., Hughes and Smith 2007) and the leaf diffusive transmittance above 620 nm (up to about 680 nm) is increasing with decreasing chlorophyll content (e.g., Lamb et al. 2002). The highest changes in the leaf transmittance related to ACN are visible around 550 nm (maximum of ACN absorption, Gitelson et al. 2001). Similar changes related to the different pigment contents were found out in the spectra of the leaf diffusive reflectance (Fig. 2c). The fact that the spectra of leaf diffusive transmittance and of leaf diffusive reflectance differ among leaves of different colorations should be manifested in SPAD and NDVI values or in other widely used optical indexes [e.g., photochemical reflectance index (PRI, Gamon et al. 1992), anthocyanins reflectance index (ARI, Gitelson et al. 2001), etc.].

The SPAD and NDVI values can be directly calculated from the leaf transmittance and reflectance according to Eqs. 10 and 24, respectively. Both SPAD and NDVI values were shown to correlate with the chlorophyll content (e.g., Gamon and Surfus 1999; Markwell et al. 1995; Nauš et al. 2010; Uddling et al. 2007). The real chlorophyll content should be read from a calibration curve (a dependence of SPAD or NDVI values on chlorophyll *a+b* content

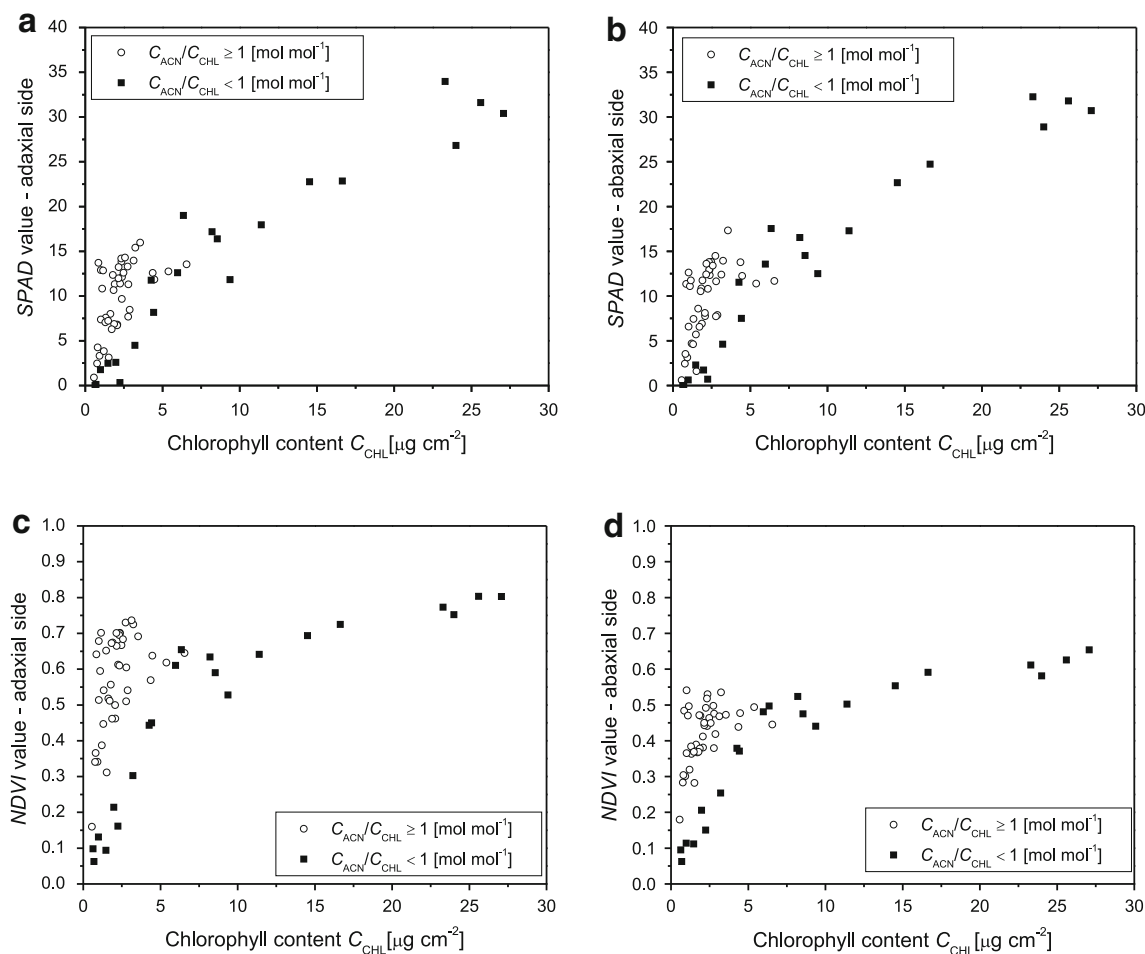


Fig. 3 A dependence of SPAD values measured from the adaxial (a) and abaxial leaf side (b) and of NDVI values measured from the adaxial (c) and abaxial leaf side (d) on chlorophyll content estimated

analytically. *Open circles* leaves with a relatively high anthocyanin content ($C_{\text{ACN}}/C_{\text{CHL}} \geq 1 \text{ mol mol}^{-1}$). *Close squares* leaves with a relatively low anthocyanin content ($C_{\text{ACN}}/C_{\text{CHL}} < 1 \text{ mol mol}^{-1}$)

estimated analytically). However, both chlorophyll meters (SPAD-502DL and Plant Pen NDVI-300) detect the leaf transmittance or leaf reflectance at wavelengths in the red part of visible light spectrum ($\lambda_{\text{IT}} = 650 \text{ nm}$ and $\lambda_{\text{IR}} = 660 \text{ nm}$, Fig. 2b, c), where they could be affected by the ACN content. Therefore, ACN-caused changes in leaf transmittance and reflectance should also be manifested in the calibration curves.

Indeed, the SPAD and NDVI reading (including the calibration curves) can differ in leaves with a different ratio of the ACN and chlorophyll content estimated analytically ($C_{\text{ACN}}/C_{\text{CHL}}$) as is shown in Fig. 3. It is obvious that similar SPAD or NDVI values can be attributed to different C_{CHL} in dependence to the ratio $C_{\text{ACN}}/C_{\text{CHL}}$ (Fig. 3). In the region of lower chlorophyll content (about 0–10 $\mu\text{g cm}^{-2}$ corresponding to partly senescent leaves), the SPAD and NDVI values measured on the leaves containing a relatively high amount of ACN ($C_{\text{ACN}}/C_{\text{CHL}} \geq 1 \text{ mol mol}^{-1}$) are higher. In some cases [particularly in dark blue leaves

(e.g., Fig. 2a, the blue leaf), where chlorophyll content is minimal] the chlorophyll meters can show exclusively the ACN content.

To show that SPAD and NDVI values can correlate with the ACN content, SPAD and NDVI values were plotted in dependence on the ACN content (Fig. 4). In case of leaves containing a relatively low amount of ACN ($C_{\text{ACN}}/C_{\text{CHL}} < 1 \text{ mol mol}^{-1}$, corresponding to closed squares in Fig. 4), the SPAD or NDVI value depends almost exclusively on chlorophyll content. However, the SPAD or NDVI value measured on the leaves containing a relatively high amount of ACN ($C_{\text{ACN}}/C_{\text{CHL}} \geq 1 \text{ mol mol}^{-1}$) correlates with ACN content. Therefore, a measurement of the SPAD or NDVI value on the leaf with $C_{\text{ACN}}/C_{\text{CHL}} \geq 1 \text{ mol mol}^{-1}$ can be used for determination of ACN content of the leaf.

Figure 5a, b shows that a reasonable limit of the ratio $C_{\text{ACN}}/C_{\text{CHL}}$ for designation of leaves containing a relatively high amount of ACN is 1 mol mol^{-1} . In the range of

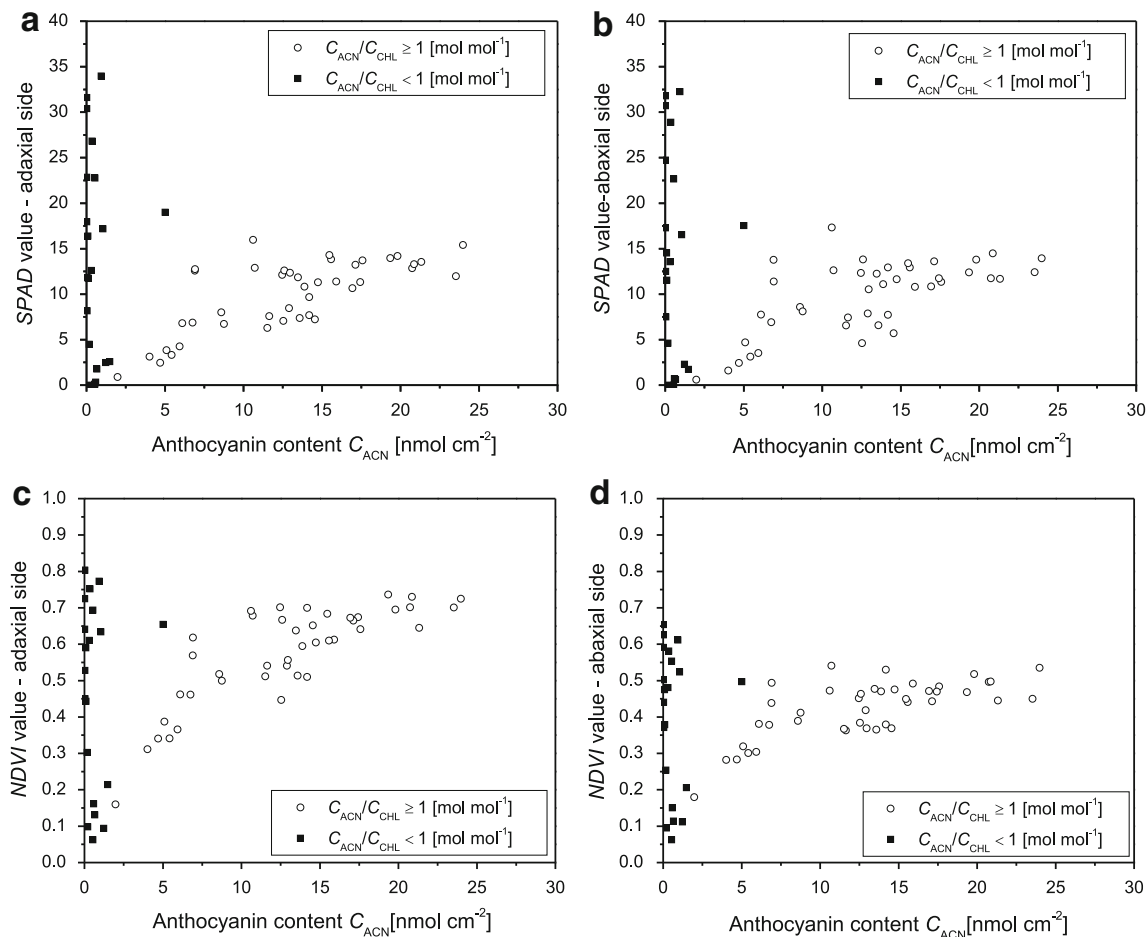


Fig. 4 A dependence of SPAD values measured from the adaxial (a) and abaxial leaf side (b) and of NDVI values measured from the adaxial (c) and abaxial leaf side (d) on anthocyanin content estimated

analytically. *Open circles* leaves with a relatively high anthocyanin content ($C_{ACN}/C_{CHL} \geq 1 \text{ mol mol}^{-1}$). *Close squares* leaves with a relatively low anthocyanin content ($C_{ACN}/C_{CHL} < 1 \text{ mol mol}^{-1}$)

C_{ACN}/C_{CHL} from 0 to about 1, the chlorophyll content is very variable (Fig. 5a) but the ACN content does not change much (points in left lower corner of Fig. 5b) with increasing C_{ACN}/C_{CHL} . However, when values of C_{ACN}/C_{CHL} are higher than about 1, the chlorophyll content is almost unchangeable (i.e., low; Fig. 5a) but ACN content increases with increasing C_{ACN}/C_{CHL} (Fig. 5b). The selected value 1 can be an interface between these two cases. The value for the interface ratio of C_{ACN}/C_{CHL} may be chosen arbitrarily in a certain interval around 1. In our case we decided to choose 1 as a well-defined ratio and well corresponding to our tests.

From the results described above, it is obvious that besides chlorophylls ACN also can contribute to the resulting leaf transmittance or reflectance at wavelengths (λ_{IT} , λ_{IR}) used by the chlorophyll meters measuring SPAD and NDVI values.

According to the “Theory” section, it is possible to obtain the spectra of calculated specific TM and RM absorbance at λ from the measured leaf transmittance and

reflectance, respectively (Eqs. 7 and 23). The spectra of $D_{sT}(\lambda)$ and $D_{sR}(\lambda)$ calculated from the representative leaf diffusive transmittance and reflectance spectra, respectively (as shown in Fig. 2b, c) are presented in Fig. 6a, b: as can be seen, ACN increased the specific absorbance in the region about 500–680 nm.

Following the method of spectral subtraction described in “Theory” section, the spectra of specific TM absorbance of chlorophyll and of ACN were obtained ($D_{Tc}(\lambda)$ and $D_{Tb}(\lambda)$). The spectra of specific TM absorbance of ACN ($D_{Tb}(\lambda)$) corresponding to the representative spectra of leaf diffusive transmittance (Fig. 2b) are shown in Fig. 6c. The $D_{Tb}(\lambda)$ spectra of leaves with the higher ACN content (the blue and blue-green leaf from Fig. 2a) evinced the peak at about 550 nm (Fig. 6c), which corresponds to the absorption spectrum of ACN in solution (e.g., Karageorgou and Manetas 2006) shifted toward to infrared region (e.g., Gitelson et al. 2001). Therefore, the ACN absorption in leaves is of non-zero value at wavelengths above 630 nm compared to a negligible ACN absorption in solution within

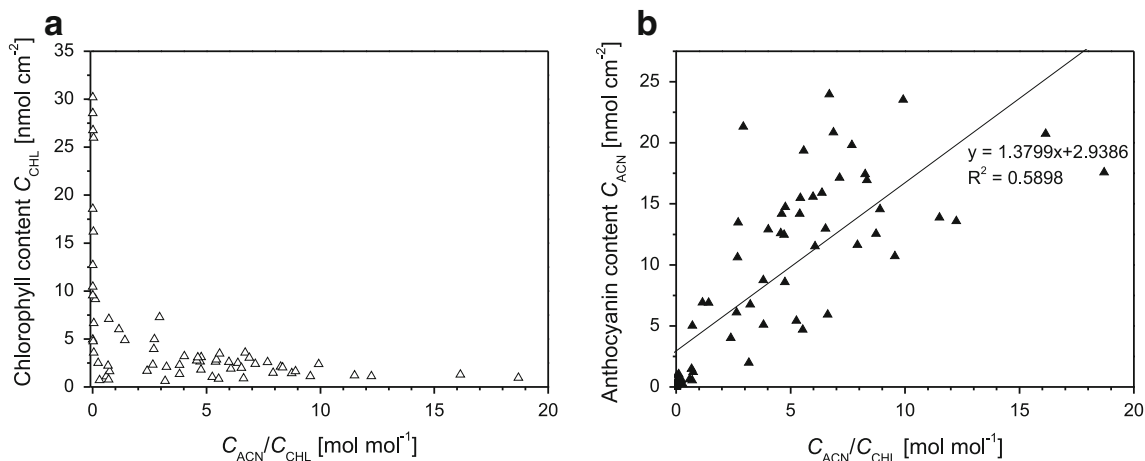


Fig. 5 The dependence of chlorophyll content (a) and anthocyanin content (b) estimated analytically on the C_{ACN}/C_{CHL} ratio of leaves estimated analytically

this region (Karageorgou and Manetas 2006). The $D_{Tb}(\lambda)$ spectra of leaves with a lower ACN content reached a local minimum (level close to zero) in region around λ_{1T} (Fig. 6c; green leaf and leaf with low pigmentation) so the ACN contribution to $D_{sT}(\lambda)$ was negligible.

The spectra of specific RM absorbance of ACN ($D_{Rb}(\lambda)$) with the shapes similar to spectra of specific TM absorbance ($D_{Tb}(\lambda)$) are shown in Fig 6d. However, the spectra of specific RM absorbance of ACN distinctively differ between adaxial and abaxial leaf side (see below).

Our results show that at the wavelength used for computing the SPAD value ($\lambda_{1T} = 650$ nm) or for computing NDVI value ($\lambda_{1R} = 660$ nm) the specific TM and RM absorbances of ACN ($D_{Tb}(\lambda_{1T})$ and $D_{Rb}(\lambda_{1R})$) have a non-zero values in the leaves containing ACN. This is one of the evidences that ACN may affect the SPAD and NDVI reading.

Spectral polarity of leaves

As mentioned above, the measured leaf diffusive transmittance from the abaxial leaf side was slightly higher compared to that from the adaxial leaf side (Fig. 2b). The spectral polarity of leaves is a consequence of different properties of the adaxial and abaxial leaf surface and adjacent cellular layers (palisade vs spongy parenchyma) including different distributions of pigments, cell shape, and intercellular spaces (Hughes and Smith 2007; Merzlyak et al. 2008; Terashima and Saeki 1983). This polarity in measured leaf diffusive transmittance spectra can lead to different measured SPAD values from adaxial and abaxial leaf side. This was manifested in the calibration curves shown in Figs. 3a, b and 4a, b.

The spectral polarity is also presented in spectra of calculated specific TM absorbance (Fig. 6a). However, as this effect is very slight, it could be neglected at least at wavelength λ_{1T} used for detection by the SPAD-502DL chlorophyll meter. Minimal differences between the spectra of calculated specific TM absorbance for the abaxial and adaxial leaf side are reflected in minimal differences between specific TM absorbance of ACN for the abaxial and adaxial leaf side (Fig. 6c). Therefore, the resulting relative contribution of ACN to the SPAD signal for the abaxial and adaxial leaf side (${}^B\Delta_b({}^B\text{SPAD})$, ${}^D\Delta_b({}^D\text{SPAD})$) should be more or less similar.

The spectral polarity of leaves was, however, more manifested in the spectra of leaf reflectance. In the spectral region 400–700 nm, the measured leaf diffusive reflectance from the abaxial leaf side was substantially higher compared to that from the adaxial leaf side (Fig. 2c). Thus, the abaxial side of tomato leaves reflected more light than the adaxial one. However, in wavelengths above 700 nm, the reflectance measured from adaxial side is higher than the reflectance measured from abaxial side. Correspondingly, the NDVI values showed in the calibration curves (Figs. 3c, d and 4c, d) are higher than NDVI values measured from abaxial side.

Since the spectra of leaf reflectance are used to obtain the spectra of calculated specific RM absorbance, the noticeable spectral polarity of leaves is maintained for the spectra of calculated specific RM absorbance (Fig. 6b) and for spectra of specific RM absorbance of ACN (Fig. 6d). As specific RM absorbances of ACN for the abaxial and adaxial leaf side are different, using these quantities in calculation of NDVI correction factor K leads to K be distinctively polar. Therefore, the NDVI correction will be dependent on the leaf side.

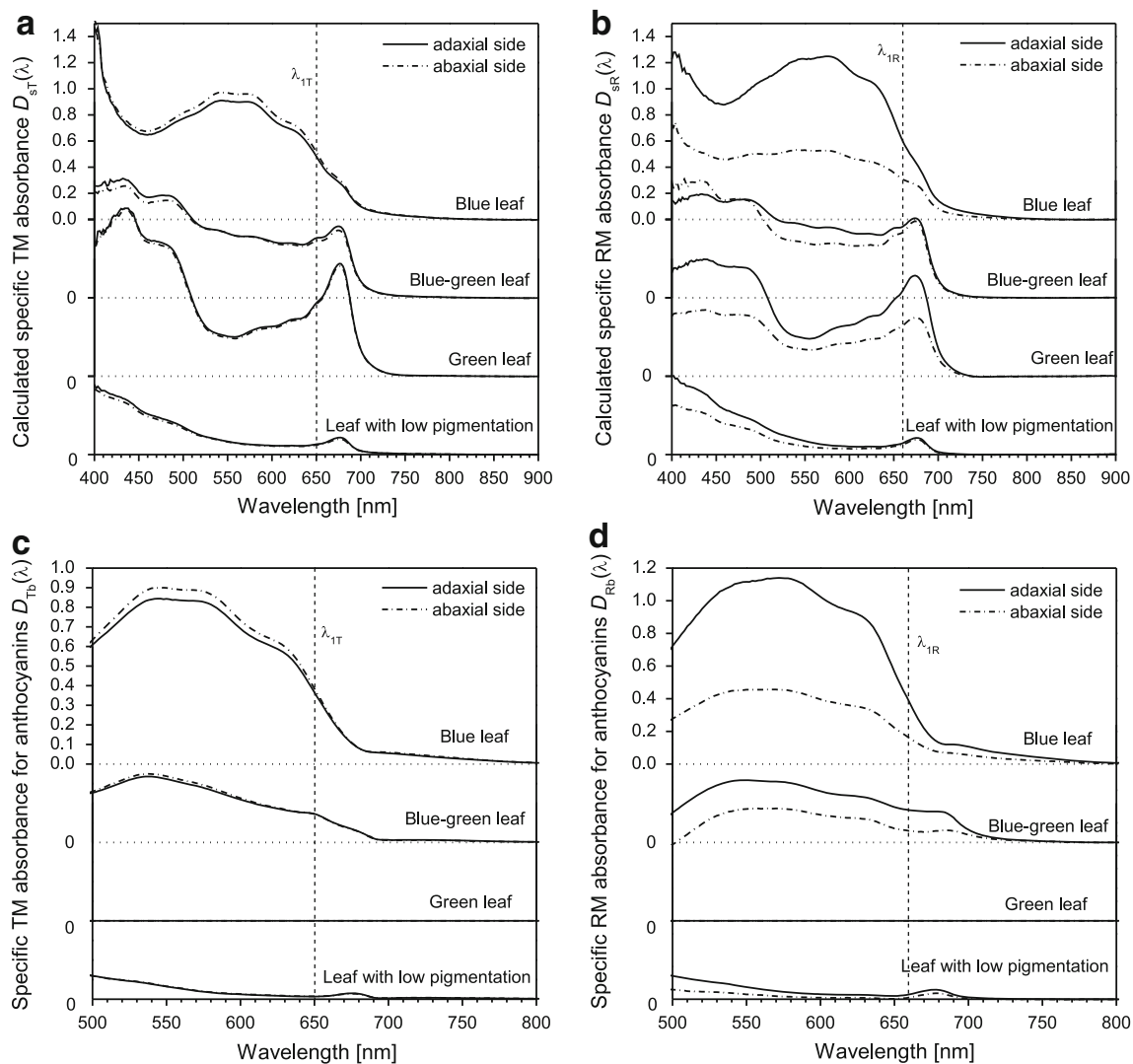


Fig. 6 Spectra of the calculated specific TM absorbance (**a**) and of calculated specific RM absorbance (**b**) of the selected leaves (see Fig. 2a) for the adaxial (*solid line*) and abaxial (*dash-dotted line*) leaf side. Spectra of the specific TM absorbance (**c**) and of the specific RM

absorbance (**d**) of anthocyanins of the selected leaves (see Fig. 2a) for the adaxial (*solid line*) and abaxial (*dash-dotted line*) leaf side obtained by the optimal spectral subtraction. The *vertical dash-dotted line* denotes the wavelength of SPAD (**a, c**) or NDVI (**b, d**) detection

Correction of the SPAD value

Drawing from the “**Theory**” section, it is possible to define the relative contribution of ACN to the specific TM absorbance at λ_{1T} ($\Delta_{Tb}(\lambda_{1T})$) (Eq. 11). Using $\Delta_{Tb}(\lambda_{1T})$, the measured SPAD value can be corrected to the ACN content in leaf (Eq. 13).

The relative contribution of ACN to the specific TM absorbance at λ_{1T} ($\Delta_{Tb}(\lambda_{1T})$) can be evaluated exclusively from the specific TM absorbance spectra of ACN or chlorophyll ($D_{Tb}(\lambda)$ and $D_{Tc}(\lambda)$; Eq. 11) calculated using the method of spectral subtraction described in “**Theory**” section. However, it is possible to obtain $\Delta_{Tb}(\lambda_{1T})$ also from the pigment content estimated analytically. Drawing

from Eq. 11 and taking into account the spectral polarity of leaves (Fig. 1a), the relative contribution of ACN to the specific TM absorbance at λ_{1T} for adaxial leaf side (${}^D\Delta_{Tb}(\lambda_{1T})$) can be rewritten as:

$${}^D\Delta_{Tb}(\lambda_{1T}) = \frac{\frac{C_{Tb}}{C_{Tc}}}{\frac{C_{Tb}}{C_{Tc}} + \frac{D_{\varepsilon_{Tc}}(\lambda_{1T})}{D_{\varepsilon_{Tb}}(\lambda_{1T})}}, \quad (33)$$

where units of concentrations are $[\text{mol l}^{-1}]$. For further calculation we expect that the ratio C_{ACN}/C_{CHL} is equal to C_{Tb}/C_{Tc} . Then Eq. 33 could be rewritten to:

$${}^D\Delta_{Tb}(\lambda_{1T}) = \frac{\frac{C_{ACN}}{C_{CHL}}}{\frac{C_{ACN}}{C_{CHL}} + \frac{D_{\varepsilon_{Tc}}(\lambda_{1T})}{D_{\varepsilon_{Tb}}(\lambda_{1T})}}, \quad (34)$$

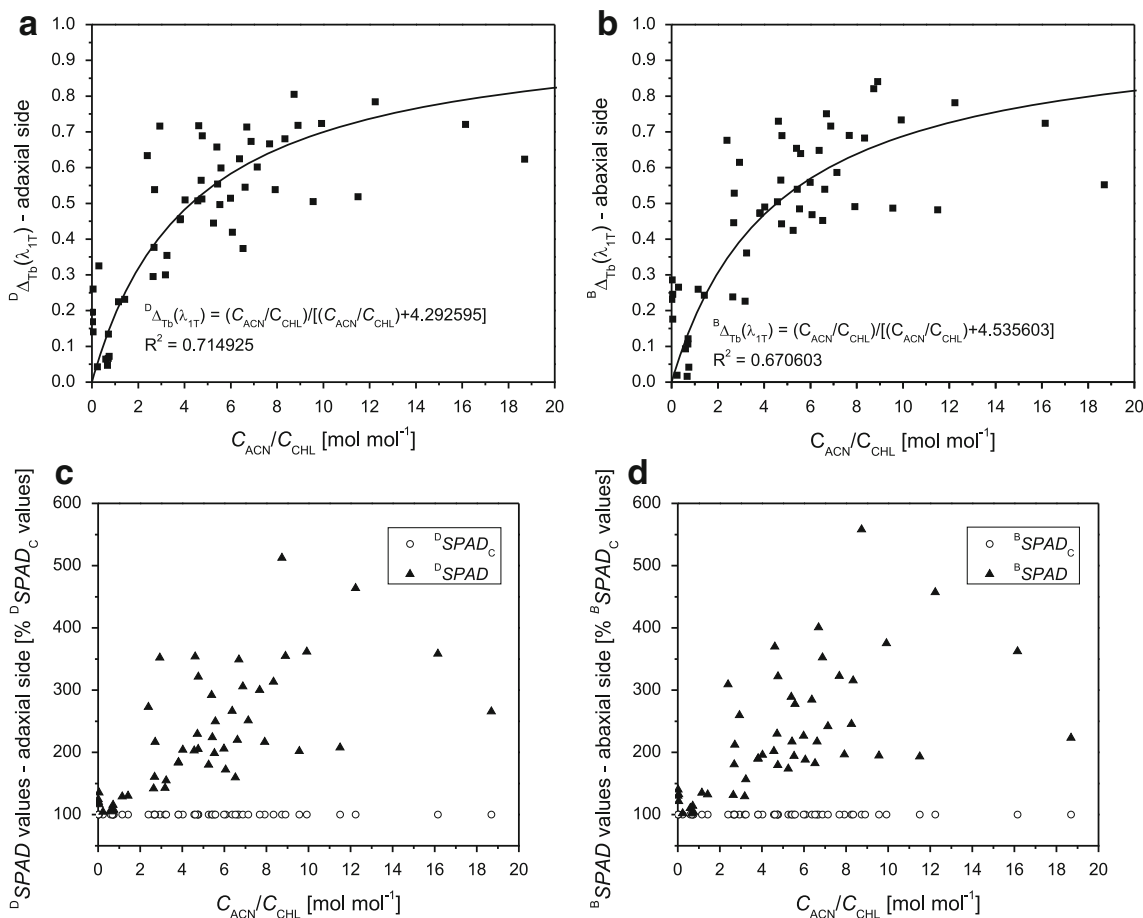


Fig. 7 A dependence of $\Delta_{Tb}(\lambda_{1T})$ (obtained by the spectral subtraction) on the C_{ACN}/C_{CHL} ratio (obtained by the analytical estimation of pigment content) for adaxial (a) and for abaxial (b) leaf side. A

dependence of the SPAD values (closed triangles) expressed in % of the corrected SPAD values (SPAD_C; open circles) on the C_{ACN}/C_{CHL} ratio for adaxial (c) and abaxial (d) leaf side

where the ratio ${}^D\varepsilon_{Tc}(\lambda_{1T})/{}^D\varepsilon_{Tb}(\lambda_{1T})$ is a constant number. For practical determination of ${}^D\Delta_{Tb}(\lambda_{1T})$, it is necessary to interconnect both approaches (using the results of spectral subtraction and analytical pigment estimation). The dependence of ${}^D\Delta_{Tb}(\lambda_{1T})$ calculated from specific absorption spectra (Eq. 11) on C_{ACN}/C_{CHL} estimated analytically is shown for our tomato leaves in Fig. 7a. Fitting the obtained dependence by Eq. 34 (a non-linear regression), the value of the ratio ${}^D\varepsilon_{Tc}(\lambda_{1T})/{}^D\varepsilon_{Tb}(\lambda_{1T})$ can be obtained.

It is now possible to propose the manner in which SPAD reading can be corrected for the ACN contribution: most generally, the dependence shown in Fig. 7a (i.e., the dependence of ${}^D\Delta_{Tb}(\lambda_{1T})$ calculated from the specific absorption spectra (Eq. 11) on C_{ACN}/C_{CHL} estimated analytically) should be measured for the selected plant species. Then, the chlorophyll *a*+*b* and ACN content of the leaf (for which the correction of SPAD value is necessary to be done) has to be estimated analytically to calculate the ratio C_{ACN}/C_{CHL} . Both the C_{ACN} and C_{CHL} should be expressed

in [nmol cm⁻²]. Subsequently, the value of the C_{ACN}/C_{CHL} ratio is used to read ${}^D\Delta_{Tb}(\lambda_{1T})$ from the analogous dependence as shown in Fig. 7a. Finally, the D SPAD_C value, corrected for the ACN contribution, has to be calculated according to Eq. 13.

The same process can be performed to have the correction of SPAD values measured from the abaxial leaf side (index B, Fig. 7b). As mentioned above, in most cases, the relative contributions of ACN to the SPAD signal for the abaxial and adaxial leaf side are very similar (they differ only within several %). Therefore, SPAD values measured from both adaxial and abaxial leaf side can be corrected by the same value of relative contribution of ACN (i.e., ${}^D\Delta_{Tb}(\lambda_{1T})$ or ${}^B\Delta_{Tb}(\lambda_{1T})$).

The ACN contribution to the SPAD reading is illustrated for both leaf sides by a percentual difference among the measured SPAD and corrected SPAD_C value (Fig. 7c, d). It can be seen that the SPAD reading may overestimate the chlorophyll content even several times in dependence on C_{ACN}/C_{CHL} for C_{ACN}/C_{CHL} higher than 1 mol mol⁻¹. With

increasing C_{ACN}/C_{CHL} , the SPAD reading is more affected by ACN content in leaves. Thus, in the case of leaves with C_{ACN}/C_{CHL} higher than 1 mol mol^{-1} the measured SPAD values should be corrected to ACN contribution according to the procedure described above.

When the analytical estimation of pigment content is not feasible, it is possible to compute $\Delta_{Tb}(\lambda_{IT})$ from the measured leaf diffusive transmittance spectrum. In this case, the spectrum of calculated specific TM absorbance ($D_{sT}(\lambda)$, Eq. 7) has to be estimated. Then the method of spectral subtraction and Eq. 11 can be used to compute $\Delta_{Tb}(\lambda_{IT})$.

Our results showing the dependence of SPAD value on the ACN content are not in accordance with Manetas et al. (1998) who concluded that the SPAD reading is not affected by ACN. The authors analyzed SPAD values and the chlorophyll and ACN content in young leaves of *Eucalyptus*, *Rosa*, and *Ricinus communis*. They found that with an increasing SPAD value the chlorophyll content increased, however, the ACN content decreased. This can be the case of young leaves of the mentioned plant species with an intensive coloration. In our study, SPAD values measured in mature green leaves of tomato were not significantly affected by ACN content. However, when mature to senescent tomato leaves with low chlorophyll content (with SPAD values below 20) were measured, ACN substantially affected the SPAD reading. Therefore, the correction of SPAD values for the ACN contribution proposed in this work should be used particularly in case of mature to partly senescent violet to blue leaves with a low amount of chlorophylls (about $0\text{--}10 \mu\text{g cm}^{-2}$).

It is relevant to note that the correction described above for the ACN contribution is not necessary to be done for some chlorophyll meters with detection wavelengths shifted toward infrared part of spectrum (e.g., 710 nm, instrument Dualex 4 Scientific (FORCE-A, Orsay, France), Cerovic et al. 2012). In case of these instruments, the detecting light is not absorbed by ACN in leaves.

Correction of NDVI value

The procedure of NDVI correction for the contribution of ACN is slightly more complicated than that described above for the SPAD values.

The NDVI value measured from the adaxial and abaxial leaf side can be corrected by the quantity K defined in Eq. 28. In the following text we focus on the adaxial leaf side, the situation on the abaxial one can be described in an analogous way. The correction of NDVI value to the ACN content using K in the case of R_c neglect is defined by Eq. 30. To compute K , it is necessary to know both ${}^D\Delta_{Rb}(\lambda_{IR})$ and ${}^D D_{sR}(\lambda_{IR})$ calculated from the leaf diffusive reflectance spectra.

Moreover, K can be calculated from the values of pigment content estimated analytically. Since the effect of spectral polarity of leaves is very significant in the leaf reflectance measurement, it is supposed that the leaf is composed of two layers with homogenous distribution of ACN and chlorophyll $a+b$: the adaxial layer (with thickness ${}^D h$ [μm]) and the abaxial layer (with thickness ${}^B h$ [μm]) (see Fig. 1a).

We suggest to use the following supposition to get expressions using only the pigment contents estimated analytically. This approximation contains a condition that the ratio of pigment content in one leaf layer to pigment content in whole leaf is the same for ACN and chlorophylls, i.e., for adaxial side, it holds:

$$\frac{{}^D C_{ACN}}{C_{ACN}} = \frac{{}^D C_{CHL}}{C_{CHL}} = d, \quad (35)$$

where ${}^D C_{ACN}$ and ${}^D C_{CHL}$ are pigment contents at the adaxial side of leaf disk that should be estimated analytically and d is a constant. However, it is not necessary to know the value of ${}^D C_{ACN}$ and ${}^D C_{CHL}$ (i.e., problematic analytical estimation of ${}^D C_{ACN}$ and ${}^D C_{CHL}$ is not needed to be done) as the constant d is a part of the factor that can be obtained by fitting procedure (see below). For abaxial side, the ratio d from Eq. 35 is designed as b .

A more exact approach not using the above approximation can be used deriving the different polarities of ACN and chlorophyll $a+b$ distribution by evaluation of the diffusive reflectance spectra. We have developed this approach (to be published elsewhere), however, it is not useful for those not having the possibility to measure the diffusive spectra.

The dependence of K on ACN and chlorophyll $a+b$ content estimated analytically is evaluated on the basis of definition of K (Eq. 28). To obtain the dependence of K on the ACN and chlorophyll $a+b$ content, the exponent of Eq. 28 (${}^D E$; product ${}^D \Delta_{Rb}(\lambda_{IR}) {}^D D_{sR}(\lambda_{IR})$) can be multiplied by 1 in form:

$$1 = \frac{({}^D C_{Rb} + {}^D C_{Rc}) \frac{1}{{}^D C_{Rc}}}{({}^D C_{Rb} + {}^D C_{Rc}) \frac{1}{{}^D C_{Rc}}} \quad (36)$$

and then ${}^D K = 10^E$, where

$${}^D E = {}^D \varepsilon_{Rb}(\lambda_{IT}) {}^D x_R \left[\frac{\frac{{}^D C_{Rb}}{{}^D C_{Rc}} ({}^D C_{Rb} + {}^D C_{Rc})}{\frac{{}^D C_{Rb}}{{}^D C_{Rc}} + 1} \right], \quad (37)$$

where the units of concentrations are [mol l^{-1}]. This form (Eq. 37) could be rewritten to the form including the obtained ACN and chlorophyll $a+b$ contents estimated analytically (C_{ACN} and C_{CHL}):

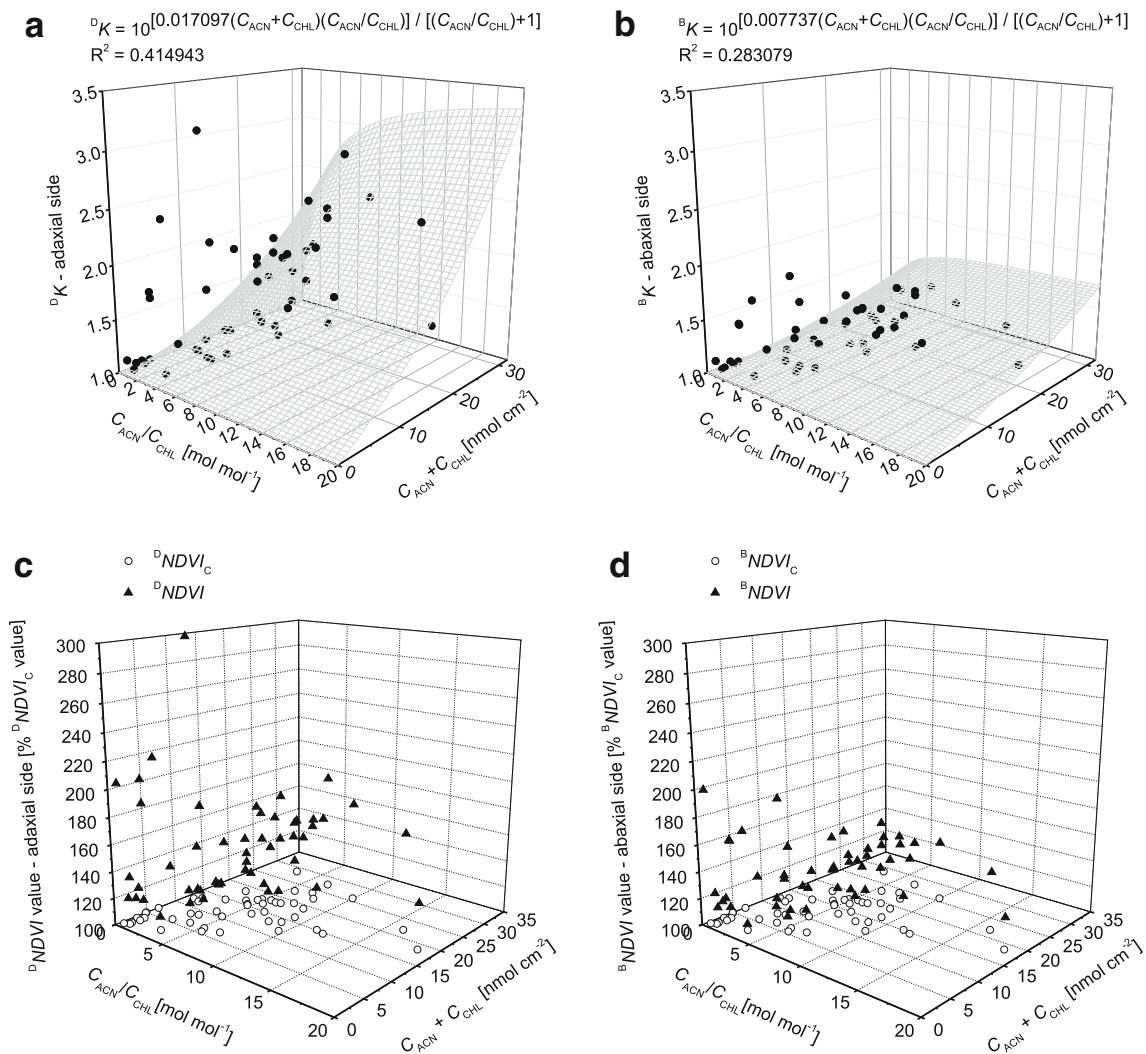


Fig. 8 A dependence of the NDVI correction factor K (obtained by the spectral subtraction) on the C_{ACN}/C_{CHL} ratio and sum $C_{ACN}+C_{CHL}$ (obtained by the analytical estimation of pigment content) for adaxial (a) and for abaxial (b) leaf side. A dependence

of the NDVI values (closed triangles) expressed in % of the corrected NDVI values ($NDVI_C$; open circles) on the C_{ACN}/C_{CHL} ratio and the sum $C_{ACN}+C_{CHL}$ for adaxial (c) and abaxial (d) leaf side

$$\begin{aligned}
 {}^D E &= \frac{{}^D \varepsilon_{Rb}(\lambda_{IT}) {}^D x_R}{{}^D h \cdot 100} \left[\frac{\frac{{}^D C_{ACN}}{{}^D C_{CHL}} ({}^D C_{ACN} + {}^D C_{CHL})}{\frac{{}^D C_{ACN}}{{}^D C_{CHL}} + 1} \right] \\
 &= \frac{{}^D \varepsilon_{Rb}(\lambda_{IT}) {}^D x_R d}{d} \left[\frac{\frac{C_{ACN}}{C_{CHL}} (C_{ACN} + C_{CHL})}{\frac{C_{ACN}}{C_{CHL}} + 1} \right].
 \end{aligned}
 \tag{38}$$

Thus, ${}^D K$ is a function of the ratio C_{ACN}/C_{CHL} and also of the sum $C_{ACN}+C_{CHL}$. A value of the ${}^D \varepsilon_{Rc}(\lambda_{IR}) \cdot {}^D x_R \cdot d / {}^D h \cdot 100$ ratio is a constant number. The depth ${}^D h$ and the number 100 are introduced to Eq. 38 to convert the units of the volume concentration to the units of area concentration (for units see the Abbreviations).

It is necessary to interconnect both approaches (using result of spectral subtraction and pigment analysis). The dependence of ${}^D K$ (calculated from spectra of ${}^D D_{Rc}(\lambda)$ and ${}^D D_{Rb}(\lambda)$) on C_{ACN}/C_{CHL} and on $C_{ACN}+C_{CHL}$ is shown for

our tomato leaves in Fig. 8a (and in Fig. 8b for abaxial side). Fitting the obtained dependence by the part of surface (graph of two-variable function defined by Eq. 38), the value of the ratio ${}^D \varepsilon_{Rc}(\lambda_{IR}) \cdot {}^D x_R \cdot d \cdot 100 / {}^D h$ can be obtained.

It is now possible to propose the manner in which NDVI reading can be corrected for the ACN contribution: most generally, the same dependence as shown in Fig. 8a [i.e., the dependence of ${}^D K$ (calculated from spectra of ${}^D D_{Rc}(\lambda)$ and ${}^D D_{Rb}(\lambda)$) on C_{ACN}/C_{CHL} and on $C_{ACN}+C_{CHL}$ estimated analytically] should be measured for the selected plant species. Then, the chlorophyll $a+b$ and ACN content in leaf (for which the NDVI correction is necessary to be done) has to be analyzed to calculate the C_{ACN}/C_{CHL} ratio and sum $C_{ACN}+C_{CHL}$. Both C_{ACN} and C_{CHL} should be expressed preferably in $[nmol\ cm^{-2}]$. Subsequently, the

values of C_{ACN}/C_{CHL} and $C_{ACN}+C_{CHL}$ estimated analytically are used to read ${}^D K$ from the same dependence as shown in Fig. 8a (for abaxial side Fig. 8b). Finally, the value $NDVI_C$, corrected for the ACN contribution, has to be calculated according to Eq. 30.

When the analytical estimation of pigment content is not feasible, it is possible to calculate ${}^D K$ from the spectra of calculated specific RM absorbance (${}^D D_{sR}(\lambda)$, Eq. 23). Then the method of spectral subtraction and Eq. 26 can be used to compute ${}^D \Delta_{RB}(\lambda_{1R})$.

The process described above was performed to correct the ACN-caused distortion of NDVI values of our tomato leaves. It is evident from Fig. 8a, b that the NDVI correction factor ${}^D K$ for adaxial side of leaves is higher than that for abaxial side of leaves. Therefore, the NDVI values measured from adaxial side of leaves should be more affected by ACN content compared to NDVI values measured from abaxial side of leaves. The percentual difference between the measured NDVI and corrected $NDVI_C$ values for tomato leaves is presented in Fig. 8c (for abaxial side Fig. 8d). Since this percentual difference depends on both C_{ACN}/C_{CHL} and sum $C_{ACN}+C_{CHL}$, the points in Fig. 8c (Fig. 8d, respectively) are not well arranged. However, it is evident that ACN contribution to NDVI values can be significant for both adaxial and abaxial side of leaves, but higher for the adaxial one. On the ground of presented results, it is recommended to correct the NDVI values measured on mature to partly senescent violet to blue leaves with a low amount of chlorophylls by the procedure described above.

The suggested correction can be used also for other indexes which could be affected by the ACN presence in leaves, i.e., those using the reflectance in a region 550–700 nm and calculated according to a formula similar to Eq. 24 [e.g., PRI (Gamon et al. 1992)].

Conclusion

This work shows that ACN can affect non-invasive optical measurement of chlorophyll *a+b* content in leaves by chlorophyll meters showing SPAD and NDVI values. The results obtained with senescing tomato leaves showed that both SPAD and NDVI values were significantly increased by the ACN presence so that the estimated chlorophyll *a+b* content was seemingly higher than the real one. Using the biophysical approach described in detail in “Theory” section, a method for correcting the readings of chlorophyll meters to eliminate ACN contributions to SPAD and NDVI measurements is proposed. Nevertheless, we recommend to determine chlorophyll content in leaves whose color is predominantly dark blue to violet (with $C_{ACN}/C_{CHL} \geq 1 \text{ mol mol}^{-1}$) by more precise analytical method.

Acknowledgements We would like to thank Eliška Ježilová for her help with measurements. This work was supported by the Ministry of Youth and Education of the Czech Republic (MSM6198959215); by the Czech Science Foundation (GD522/08/H003); and by the Grant no. ED0007/01/01 Centre of the Region Haná for Biotechnological and Agricultural Research.

References

- Albert NW, Lewis DH, Zhang H, Irving LJ, Jameson PE, Davies KM (2009) Light-induced vegetative anthocyanin pigmentation in petunia. *J Exp Bot* 60:2191–2202
- Atlassi Pak V, Nabipour M, Meskarbashee M (2009) Effect of salt stress on chlorophyll content, fluorescence, Na^+ and K^+ ions content in rape plants (*Brassica napus* L.). *Asian J Agric Res* 3:28–37
- Cerovic ZG, Masdoumier G, Ghazlen NB, Latouche G (2012) A new optical leaf-clip meter for simultaneous non-destructive assessment of leaf chlorophyll and epidermal flavonoids. *Physiol Plantarum* 146:251–260
- Chalker-Scott L (1999) Environmental significance of anthocyanins in plant stress responses. *Photochem Photobiol* 70:1–9
- Close DC, Beadle CL (2003) The ecophysiology of foliar anthocyanin. *Bot Rev* 69:149–161
- Coste S, Baraloto C, Leroy C, Marcon É, Renaud A, Richardson AD, Roggy J-C, Schimann H, Uddling J, Hérault B (2010) Assessing foliar chlorophyll contents with the SPAD-502DL chlorophyll meter: a calibration test with thirteen tree species of tropical rainforest in French Guiana. *Ann For Sci* 67:607
- Feild TS, Lee DW, Holbrook NM (2001) Why leaves turn red in autumn. The role of anthocyanins in senescing leaves of red-osier dogwood. *Plant Physiol* 127:566–574
- Gamon JA, Surfus JS (1999) Assessing leaf pigment content and activity with a reflectometer. *New Phytol* 143:105–117
- Gamon JA, Peñuelas J, Field CB (1992) A narrow-waveband spectral index that tracks diurnal changes in photosynthetic efficiency. *Remote Sens Environ* 41:35–44
- Gauche C, Malagoli ED, Luiz MTB (2010) Effect of pH on the copigmentation of anthocyanins from Cabernet Sauvignon grape extracts with organic acids. *Sci Agric* 67:41–46
- Gitelson AA, Merzlyak MN, Chivkunova OB (2001) Optical properties and nondestructive estimation of anthocyanin content in plant leaves. *Photochem Photobiol* 74:38–45
- Gitelson AA, Peng Y, Masek JG, Rundquist DC, Verma S, Suyker A, Baker JM, Hatfield JL, Meyers T (2012) Remote estimation of crop gross primary production with Landsat data. *Remote Sens Environ* 121:404–414
- Giusti MM, Wrolstad RE (2001) Characterization and measurement of anthocyanins by UV-visible spectroscopy. *Curr Protoc Food Analyt Chem* F1.2.1–F1.2.13
- Guo J, Wang M-H (2010) Ultraviolet A-specific induction of anthocyanin biosynthesis and PAL expression in tomato (*Solanum lycopersicum* L.). *Plant Growth Regul* 62:1–8
- Hoch WA, Zeldin EL, McCown BH (2001) Physiological significance of anthocyanins during autumnal leaf senescence. *Tree Physiol* 21:1–8
- Hörtensteiner S (2006) Chlorophyll degradation during senescence. *Annu Rev Plant Biol* 57:55–77
- Hughes NM, Smith WK (2007) Attenuation of incident light in *Galax urceolata* (Diapensiaceae): concerted influence of adaxial and abaxial anthocyanic layers on photoprotection. *Am J Bot* 94:784–790
- Jifon JL, Syvertsen JP, Whaley E (2005) Growth environment and leaf anatomy affect nondestructive estimates of chlorophyll and nitrogen in *Citrus* sp. leaves. *J Amer Soc Hort Sci* 130:152–158

- Junka N, Kanlayanarat S, Buanong M, Wongs-Aree C (2012) Characterisation of floral anthocyanins and their antioxidant activity in *Vanda* hybrid (*V. teres* x *V. hookeriana*). *J Food Agric Environ* 10:221–226
- Karageorgou P, Manetas Y (2006) The importance of being red when young: anthocyanins and the protection of young leaves of *Quercus coccifera* from insect herbivory and excess light. *Tree Physiol* 26:613–621
- Kytridis V-P, Manetas Y (2006) Mesophyll versus epidermal anthocyanins as potential in vivo antioxidants: evidence linking the putative antioxidant role to the proximity of oxy-radical source. *J Exp Bot* 57:2203–2210
- Lamb DW, Steyn-Ross M, Schaare P, Hanna MM, Silvester W, Steyn-Ross A (2002) Estimating leaf nitrogen concentration in ryegrass (*Lolium* spp.) pasture using the chlorophyll red-edge: theoretical modelling and experimental observations. *Int J Remote Sens* 23:3619–3648
- Leyva A, Jarillo JA, Salinas J, Martinez-Zapater JM (1995) Low temperature induces the accumulation of phenylalanine ammonia-lyase and chalcone synthase mRNAs of *Arabidopsis thaliana* in a light-dependent manner. *Plant Physiol* 108:39–46
- Lichtenthaler HK (1987) Chlorophyll and carotenoids: pigments of photosynthetic biomembranes. *Methods Enzymol* 148:350–382
- Loh FCW, Grabosky JC, Bassuk NL (2002) Using the SPAD 502 meter to assess chlorophyll and nitrogen content of benjamin fig and cottonwood leaves. *Hort Technol* 12:682–686
- Manetas Y, Grammatikopoulos G, Kyparissis A (1998) The use of the portable, non-destructive, SPAD-502DL (Minolta) chlorophyll meter with leaves of varying trichome density and anthocyanin content. *J Plant Physiol* 53:513–516
- Markwell J, Osterman JC, Mitchell JL (1995) Calibration of the Minolta SPAD-502DL leaf chlorophyll meter. *Photosynth Res* 46:467–472
- McClendon JH, Fukshansky L (1990) On the interpretation of absorption-spectra of leaves. 1. Introduction and the correction of leaf spectra for surface reflection. *Photochem Photobiol* 51:203–210
- Mendez M, Jones DG, Manetas Y (1999) Enhanced UV-B radiation under field conditions increases anthocyanin and reduces the risk of photoinhibition but does not affect growth in the carnivorous plant *Pinguicula vulgaris*. *New Phytol* 144:275–282
- Merzlyak MN, Chivkunova OB, Solovchenko AE, Naqvi KR (2008) Light absorption by anthocyanins in juvenile, stressed, and senescing leaves. *J Exp Bot* 59:3903–3911
- Nauš J, Rolencová M, Hlaváčková V (2008) Is chloroplast movement in tobacco plants influenced systemically after local illumination or burning stress? *J Integr Plant Biol* 50:1292–1299
- Nauš J, Prokopová J, Řebíček J, Špundová M (2010) SPAD chlorophyll meter reading can be pronouncedly affected by chloroplast movement. *Photosynth Res* 105:265–271
- Pietrini F, Iannelli MA, Massacci A (2002) Anthocyanin accumulation in the illuminated surface of maize leaves enhances protection from photo-inhibitory risks at low temperature, without further limitation to photosynthesis. *Plant Cell Environ* 25:1251–1259
- Qin C, Li Y, Niu W, Ding Y, Zhang R, Shang X (2010) Analysis and characterisation of anthocyanins in mulberry fruit. *Czech J Food Sci* 28:117–126
- Sheoran IS, Dumonceaux T, Datla R, Sawhney VK (2006) Anthocyanin accumulation in the hypocotyl of an ABA-over producing male-sterile tomato (*Lycopersicon esculentum*) mutant. *Physiol Plant* 127:681–689
- Sims DA, Gamon JA (2002) Relationships between leaf pigment content and spectral reflectance across a wide range of species, leaf structures and developmental stages. *Remote Sens Environ* 81:337–354
- Solovchenko AE, Chivkunova OB (2011) Physiological role of anthocyanin accumulation in common hazel juvenile leaves. *Russ J Plant Physiol* 58:674–680
- Tanaka Y, Sasaki N, Ohmiya A (2008) Biosynthesis of plant pigments: anthocyanins, betalains and carotenoids. *Plant J* 54:733–749
- Terashima I, Saeki T (1983) Light environment within a leaf I. optical properties of paradermal sections of *Camellia* leaves with special reference to differences in the optical properties of palisade and spongy tissues. *Plant Cell Physiol* 24:1493–1501
- Uddling J, Gelang-Alfredsson J, Piikki K, Pleijel H (2007) Evaluating the relationship between leaf chlorophyll concentration and SPAD-502DL chlorophyll meter readings. *Photosynth Res* 91:37–46